AD-A045 903 TEMPLE UNIV PHILADELPHIA PA F/G 7/4

STRUCTURE-PROPERTY RELATIONSHIPS IN ALIGNED CHIRAL NEMATIC PHAS--ETC(U)

SEP 77 M M LABES DAHC04-74-G-0186

UNCLASSIFIED ARO-12041.1-C NL

1 OF 1
ADA
045903

END
DATE
FILMED
11-77
DDC

(18) Unclassified

SECURITY CLASSIFICATION OF THIS PAGE (When Data Entered)

(12) ARO 12041.1-C

ADA045903

(1) ARO REPORT DOCUMENTATION PAGE		READ INSTRUCTIONS BEFORE COMPLETING FORM
1. REPORT NUMBER (19) 12041.1-C	2. GOVT ACCESSION NO.	3. RECIPIENT'S CATALOG NUMBER
4. TITLE (and Subtitle) (6) Structure-Property Relationships in Aligned Chiral Nematic Phases		5. TYPE OF REPORT & PERIOD COVERED (9) Final Report, 1 Jun 74 — 31 Aug 77
		6. PERFORMING ORG. REPORT NUMBER
7. AUTHOR(s) (10) M. M. Labes		8. CONTRACT OR GRANT NUMBER(s) (15) DAHC04-74-G-0186 new
9. PERFORMING ORGANIZATION NAME AND ADDRESS Temple University Philadelphia, Pennsylvania 19122		10. PROGRAM ELEMENT, PROJECT, TASK AREA & WORK UNIT NUMBERS (11)
11. CONTROLLING OFFICE NAME AND ADDRESS U. S. Army Research Office Post Office Box 12211 Research Triangle Park, NC 27709		12. REPORT DATE Sep 77
		13. NUMBER OF PAGES 5
14. MONITORING AGENCY NAME & ADDRESS (if different from Controlling Office) (12) 46p.		15. SECURITY CLASS. (of this report) Unclassified
		15a. DECLASSIFICATION/DOWNGRADING SCHEDULE

16. DISTRIBUTION STATEMENT (of this Report)

Approved for public release; distribution unlimited.

17. DISTRIBUTION STATEMENT (of the abstract entered in Block 20, if different from Report)

18. SUPPLEMENTARY NOTES

The findings in this report are not to be construed as an official Department of the Army position, unless so designated by other authorized documents.

19. KEY WORDS (Continue on reverse side if necessary and identify by block number)

Structure	Solutes	Fluorescence
Diffusion	Solvents	
Liquid crystals	Mixtures	
Molecular properties	Pyroelectric effect	

20. ABSTRACT (Continue on reverse side if necessary and identify by block number)

The purpose of this grant was to explore structure-property relationships in aligned chiral nematic (liquid crystalline) phases. Much basic information was missing: and for example, the speed at which ~~how rapidly do~~ molecules diffuse in a liquid crystalline phase, and the ~~What~~ aspects of molecules' size, shape and functionality affect the molecular "twisting power" of solute molecules in chiral liquid crystalline solvents? What factors define the defect structure of liquid crystalline samples? All of these questions were examined during the course of this grant.

DD FORM 1 JAN 73 1473 EDITION OF 1 NOV 65 IS OBSOLETE

346350

Unclassified

SECURITY CLASSIFICATION OF THIS PAGE (When Data Entered)

20 COPIES REQUIRED

PROGRESS REPORT

FINAL REPORT

1. ARO PROPOSAL NUMBER: 12041c

2. PERIOD COVERED BY REPORT: June 1, 1974 - August 31, 1977

3. TITLE OF PROPOSAL: Structure-Property Relationships in Aligned Chiral Nematic Phases

4. CONTRACT OR GRANT NUMBER: DAHC04-74-G-0186

5. NAME OF INSTITUTION: Temple University

6. AUTHOR(S) OF REPORT: M. M. Labes

7. LIST OF MANUSCRIPTS SUBMITTED OR PUBLISHED UNDER ARO SPONSORSHIP DURING THIS PERIOD, INCLUDING JOURNAL REFERENCES:

SEE ATTACHED LIST

8. SCIENTIFIC PERSONNEL SUPPORTED BY THIS PROJECT AND DEGREES AWARDED DURING THIS REPORTING PERIOD:

C. S. Bak -- Post-Doctoral Research Associate
A. E. Stieb -- Post-Doctoral Research Associate
H. Hakemi -- Graduate Research Assistant (Ph.D. awarded January 1976)
J. W. Park -- Graduate Research Assistant (Ph.D. awarded January 1977)
L. J. Yu -- Graduate Research Assistant (Ph.D. expected January 1978)
A. Hochbaum -- Graduate Research Assistant

ARO Form 129
18 Sep 75

BRIEF OUTLINE OF RESEARCH FINDINGS

The purpose of this grant was to explore structure-property relationships in aligned chiral nematic (liquid crystalline) phases. Much basic information was missing: for example, how rapidly do molecules diffuse in a liquid crystalline phase? What aspects of molecules' size, shape and functionality affect the molecular "twisting power" of solute molecules in chiral liquid crystalline solvents? What factors define the defect structure of liquid crystalline samples? All of these questions were examined during the course of this grant, and the following results were obtained.

Diffusion in Liquid Crystals:

An optical method for determining diffusion coefficients and their anisotropy was developed and applied to several systems. See papers (1) and (6) listed below.

Analyses of Pitch Concentration Dependences in Multicomponent Liquid Crystal Mixtures:

A general equation was developed in which pitch in a mixture of liquid crystals is expressed as a quadratic function of the number densities of component molecules of given molecular twisting powers. The equation successfully treats and is predictive of twisting power over the entire phase diagram of binary and ternary liquid crystal systems. See papers (2) and (3) listed below.

Molecular Twisting Power Anomalies:

A literature report of an unusually large twisting power of a non-mesogenic solute was shown to be incorrect. The effect is due to a chemical

reaction between solute and solvent. See paper (5) listed below.

Texture and Disclinations in Nematic and Cholesteric Liquid Crystals:

An attempt was made to understand structurally the reasons for the various textures observed in liquid crystal films as well as their defect structures, including the development of a description of a new theoretical generation process for disclinations of integer strength. See papers (8) and (11) listed below.

Several other investigations relating to the phase diagrams, electronic, and electro-optic properties of liquid crystals were also undertaken during the course of this grant.

Study of Molecular Complexing in Liquid Crystals:

It was discovered that mixing liquid crystal binaries from donor- and acceptor-like materials leads to unusual phase diagrams -- double eutectics, increases in nematic-isotropic phase transition temperatures, non-linear dielectric properties, and desirable electro-optic performance characteristics. See papers (4), (9) and (10) listed below.

Pyroelectric Effect in Chiral Smectic C and H Liquid Crystals: (partial support)

The ferroelectric-like structure of the chiral smectic C and H phases was confirmed by the experimental observation of a pyroelectric effect. See paper (7) listed below.

Fluorescent Liquid Crystal Display:

An electric field-induced cholesteric-nematic transition on a sample containing a europium chelate guest molecule of little or no polarization shows contrast ratios as high as 9:1 for its brilliant red (612 nm) fluorescence. See paper (12) listed below.

LIST OF MANUSCRIPTS SUBMITTED OR PUBLISHED UNDER ARO SPONSORSHIP DURING THIS PERIOD, INCLUDING JOURNAL REFERENCES:

(1) H. Hakemi and M. M. Labes, "New Optical Method for Studying Anisotropic Diffusion in Liquid Crystals", J. Chem. Phys. 61, 4020 (1974).

(2) C. S. Bak and M. M. Labes, "Pitch-Concentration Relationships in Multi-Component Liquid Crystal Mixtures", J. Chem. Phys. 62, 3066 (1975).

(3) C. S. Bak and M. M. Labes, "Analysis of Pitch-Concentration Dependences in Some Binary and Ternary Liquid Crystal Mixtures", J. Chem. Phys. 63, 805 (1975).

(4) J. W. Park, C. S. Bak and M. M. Labes, Effects of Molecular Complexing on the Properties of Binary Nematic Liquid Crystal Mixtures", J. Amer. Chem. Soc. 97, 4398 (1975).

(5) J. W. Park and M. M. Labes, "On the Helical Twisting Power of α-Phenethylamine in Nematic Liquid Crystals", Mol. Cryst. Liq. Cryst. 31, 355 (1975).

(6) H. Hakemi and M. M. Labes, "Self-Diffusion Coefficients of a Nematic Liquid Crystal via an Optical Method", J. Chem. Phys. 63, 3708 (1975).

(7) L. J. Yu, H. Lee, C. S. Bak and M. M. Labes, "Observation of Pyroelectricity in Chiral Smectic C and H Liquid Crystals", Phys. Rev. Lett. 36, 388 (1976). (partial support).

(8) A. E. Stieb and M. M. Labes, "Electric Field Induced Transformation and Structural Explanations of Large Pitch Cholesteric Fingerprint and Spherulitic Textures". Presented at the Kent State Liquid Crystal Conference, August 1976, Abstract #C1-13.

(9) J. W. Park and M. M. Labes, "Dielectric, Elastic and Electro-Optic Properties of a Liquid Crystalline Molecular Complex", J. Appl. Phys. 48, 22 (1977).

(10) J. W. Park and M. M. Labes, "Broadening of the Nematic Temperature Range by a Non-Mesogenic Solute in a Nematic Liquid Crystal", Mol. Cryst. Liq. Cryst. Letters 34, 147 (1977).

(11) A. E. Stieb and M. M. Labes, "A New Generation Process and Matrix Representation of Disclinations in Nematic and Cholesteric Liquid Crystals", Mol. Cryst. Liq. Cryst. (accepted). Also presented at the Kent State Liquid Crystal Conference, August 1976, Abstract #C1-15.

(12) L. J. Yu and M. M. Labes, "Fluorescent Liquid Crystal Display Utilizing an Electric Field Induced Cholesteric-Nematic Transition", Appl. Phys. Lett. (submitted).

New optical method for studying anisotropic diffusion in liquid crystals*

H. Hakemi and M. M. Labes

Department of Chemistry, Temple University, Philadelphia, Pennsylvania 19122
(Received 7 June 1974)

A new approach to studying diffusion in liquid crystals is described in which the optically observable textural changes in a nematic phase caused by a cholesteric diffusant gives direct visualization of the concentration gradient. Utilizing either homeotropic of homogeneous alignments under different boundary conditions, and with and without an applied magnetic field, the parallel and perpendicular components of the diffusivity have been determined for a cholesteryl ester diffusing into *N*-(*p*-methoxybenzylidene)-*p*-*n*-butylaniline as a function of temperature. The diffusion coefficients in the isotropic phase can also be determined by annealing at a high temperature and quenching to room temperature, whereupon the cholesteric texture is again developed. Values of the diffusion coefficients and the activation energies of the diffusion process are discussed and compared to other available data.

INTRODUCTION

Although the very name "liquid crystals" identifies a basic property of flow while orientational order is maintained, the nature of this flow on a microscopic basis is not well understood. Progress has been made in relating experimentally determined viscosity coefficients to continuum theory,[1] but little progress has been made in understanding diffusion processes in these systems. Where experimental data on diffusion do exist, they are not consistent from method to method, nor with viscosity data.

This lack of progress is somewhat surprising, since Svedberg first recognized the importance of measuring diffusion coefficients in liquid crystals many years ago and studied magnetic field effects on rates of diffusion[2] and rates of reaction[3,4] in liquid crystal phases. He was fascinated by being able to control diffusivity and reactivity in these phases.

The significance of the problem may also be viewed in terms of the current use of liquid crystalline phases as models for biological ordering. That biological systems are replete with liquid crystalline materials has been frequently reported. For example, Stewart[5] showed that complex lipids present in the adrenal cortex, ovaries, and myelin exist at body temperatures in a characteristic mesophase. Robinson[6] has shown a widespread occurrence of the cholesteric phase in polypeptide solutions and biological structures. In earlier work, we suggested that liquid crystalline orientation in a magnetic field might offer a possible explanation for some of the rather controversial effects reported for magnetic fields acting on biological systems.[7] The occurrence of mesoforms in membrane structures,[8] the known response of lyotropic,[9] nematic,[10] and cholesteric[11] phases to magnetic fields, led us to study the change of diffusion rates through a thin liquid crystal "membrane" by a magnetic field,[12] and indeed such changes were noted.

There has been only one attempt to develop a theory of diffusion in mesophases.[13] Experimental approaches include quasielastic scattering of cold neutrons,[14-17] proton spin echo methods,[14,18-23] and radioactive tracer techniques for both self-[24] and impurity[12] diffusion. Results to date have indicated difficulties and inconsistencies in the methodologies employed. For example, in the isotropic phase of *p*-azoxyanisole (PAA), values as low[24] as 4.1×10^{-6} cm^2 sec^{-1} and as high[17,22] as 1.7×10^{-5} cm^2 sec^{-1} have been reported for the self-diffusion coefficient. Values for $D_\parallel$ in the nematic phase of PAA as high[17] as 2×10^{-5} cm^2 sec^{-1} and as low[24] as 4.1×10^{-6} cm^2 sec^{-1} are also reported. Results with *N*-(*p*-methoxybenzylidene)-*p*-*n*-butylaniline (MBBA) are also inconsistent.

In this paper, we report a totally different approach to studying diffusion in liquid cyrstals in which the optically observable textural changes in a nematic liquid crystal caused by a cholesteric diffusant give direct visualization of the concentration gradient. The method is both conceptually and experimentally simple; it readily lends itself to studying the anisotropic components of the diffusivity in both cholesteric and nematic systems as well as diffusion in the isotropic phase. Data are presented for a cholesteryl ester, cholesteryl-(−)(*R*)-2-methylvalerate (CMV), diffusing into MBBA. Several boundary conditions are employed, and the data are shown to be self-consistent.

EXPERIMENTAL

Materials

CMV was prepared as previously described.[25] The optical purity of the ester was determined by an NMR method utilizing the lanthanide shift reagent Eu(DPM)$_3$, and found to be $91\pm1\%$. MBBA was obtained from Eastman Kodak Co. in a pure grade sealed in septum bottles under nitrogen (Eastman X11246). A solution of CMV in MBBA was used as the diffusant source into MBBA samples which were carefully aligned by wall effects in the manner described below.

Homogeneously aligned nematic

MBBA was placed between two silicon monoxide coated glass plates[26] separated by a mylar spacer, typically 12.7 μm thick. With the plates properly coated and oriented, a uniaxial alignment can be achieved, in which the molecular axis is parallel to the glass walls, the so-called homogeneous alignment. The mylar spacer was

cut so as to provide a rectangular path ~0.2 cm wide and 1 cm long. A thin strip (~0.05 cm) of diffusant mixture was placed along the edge of the top glass plate and allowed to diffuse linearily into the rectangular path. Figure 1 is a photograph of the observed texture of the MBBA after diffusion has occurred, developing lines reminiscent of the Grandjean structure in cholesteric liquid crystals.[27]

Homeotropically aligned nematic

MBBA is placed between two lecithin coated glass plates,[28] giving the homeotropic alignment in which the molecular axis is perpendicular to the glass walls. If coatings are prepared by dipping the plates in a dilute chloroform solution of lecithin, no rubbing is required to achieve well-oriented samples. Linear diffusion experiments were conducted in an exactly analogous manner to the homogeneous case, and Fig. 2 is a photograph of the observed texture after diffusion has occurred. The pattern developed is the fingerprint texture of cholesteric liquid crystals.[29] The size of the fingerprint is related to the pitch of the helical array, which in turn depends on the concentration of CMV in MBBA. Alternately, two round glass plates ~$1\frac{1}{4}$ in. in diameter were used with the top plate drilled with an 0.06 cm diameter hole. The diffusant was injected into the hole and allowed to diffuse radially, producing similar patterns to that shown in Fig. 2.

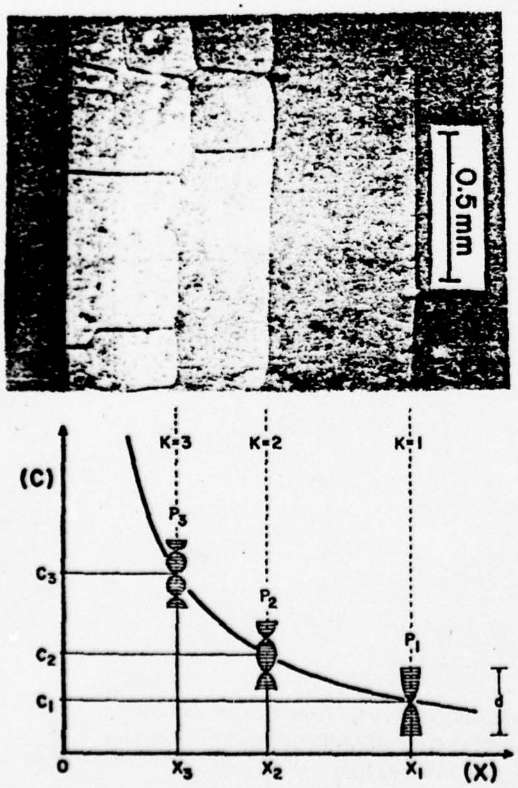

FIG. 1. Diffusion pattern for CMV in a 12.7 μm sample of homogeneously aligned MBBA at 22°. When $P_N/2$ is an integral multiple of the thickness, a Grandjean line appears. Diffusant source is at the left of the photograph.

FIG. 2. Diffusion pattern for CMV in a 12.7 μm sample of homeotropically aligned MBBA of 22°. Diffusant source is at the bottom of the photograph.

Experimental procedure

Glass sandwiches were placed in either a Unitron Hot Stage or a brass cell through which liquid from a constant temperature bath was circulated, providing ±0.25° temperature control. The brass cell design has been described previously.[30] The diffusion gradients were photographed through a Nikon LKE microscope with crossed polarizers at 25–300 times magnification. The brass cell could also be placed in the gap of a 9 in. electromagnet and a field of 10 000 Oe applied either parallel or perpendicular to the original molecular axis alignment. In the isotropic region, the samples were held at the anneal temperature and then quenched rapidly to room temperature, whereupon the liquid crystal texture developed.

The initial concentration of CMV in MBBA was varied in the range 5%–50% by weight, most experiments being conducted at the 5% level. Thickness of the samples was varied from 6.3–36.5 μ. Anneal times varied from ~3 to 5 h in the isotropic phase to ~1.5 to 3 days in the nematic phase. There was no observable effect of these three variables on the values of the diffusion coefficients within the experimental error.

Pitch-concentration relationship

For the homeotropically aligned nematic, where a fingerprint texture is observed, one expects a plot of pitch^{-1} vs concentration to be linear at low concentrations, provided the sample thickness is much greater than the pitch.[29] When pitch becomes larger than or comparable to thickness, difficulties are encountered, because wall effects cause considerable tilt in the helicoidal arrays. A determination was therefore made of the precise pitch–concentration relationship over the entire range of concentrations used in the diffusion experiments and is given in Fig. 3; concentration data

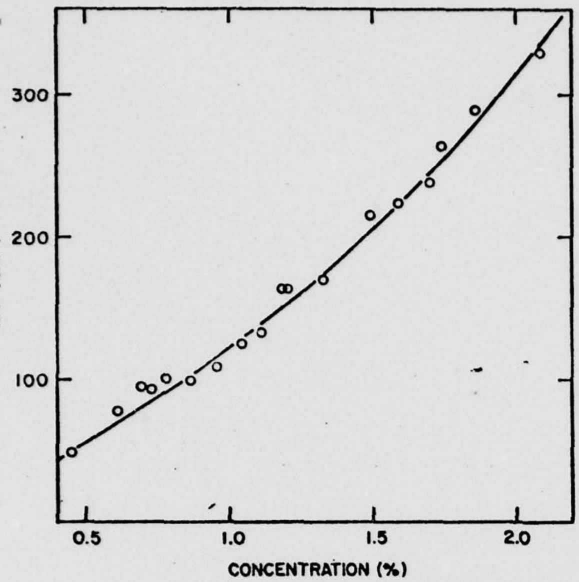

FIG. 3. Reciprocal pitch (cm^{-1}) vs concentration (weight %) of CMV in MBBA at 24.5°. Sample thickness is 12.7 μm.

were corrected for the nonlinearity of this curve, where necessary.

RESULTS

Diffusion into homogeneously aligned nematic

When a cholesteric diffusant establishes a concentration gradient in a homogeneously aligned nematic phase, a pattern of Grandjean lines is established similar to those observed in a wedge-shaped space confining a cholesteric liquid crystal.[27] The Grandjean lines arise at equidistant intervals where the gap in the wedge is a multiple integer of the half-pitch. As is shown in Fig. 1, when an exponential concentration gradient is created by the diffusion process in a fixed thickness sample, there should be distances at which the thickness is again a multiple integer of the half-pitch, but these distances are variable. At fixed thickness d, pitch P_k then has values according to the relationship

$$d=\frac{k}{2}P_k \ , \tag{1}$$

where k is an integer ($k=1,2,3,\ldots$).

For diffusion from a semi-infinite line source into a plane surface, the appropriate solution of Fick's law is given by[30]

$$C=\frac{M}{(\pi Dt)^{1/2}}\exp(-x^2/4Dt) \ , \tag{2}$$

where C is the concentration of the diffusant at a distance x from the source at time t, M is the total amount of material diffusing, and D is the concentration-independent diffusion coefficient. The concentration in the experiment can be related to the pitch P_k of the helical array; at low concentrations, there is a linear relationship

$$C_k=\gamma/P_k \ . \tag{3}$$

By substituting (1) and (3) into the diffusion equation (2), one obtains

$$k=\frac{2dM}{\gamma(\pi Dt)^{1/2}}\exp(-x_k^2/4Dt) \ . \tag{4}$$

Thus, by simply measuring values of x_k at a time t, one can determine the diffusion coefficient D from the equation

$$\ln k=\text{const}-x_k^2/4Dt \ . \tag{5}$$

It would obviously be best to develop the diffusion pattern until a large number of Grandjean type lines appeared and graphically evaluate Eq. (5) from a plot of $\ln k$ vs x_k^2. In most of our experiments, when the initial diffusant concentration is low, only two or three k values could be observed, and hence the determination of D was done by calculating the slope of the $\ln k$ vs x_k^2 relationship from only two or three points.[31]

In this configuration, the diffusant is entering a matrix in which the long axes of the molecules are all parallel to the diffusing path, so that one is effectively determining $D_\parallel$. Values determined in this way are plotted in Fig. 4 at several temperatures in the nematic phase. It can be seen that $D_\parallel$ is only very slightly temperature dependent.

To verify that the molecular alignment caused by wall effects is essentially complete and that the helical orientations created in the diffusion process do not appre-

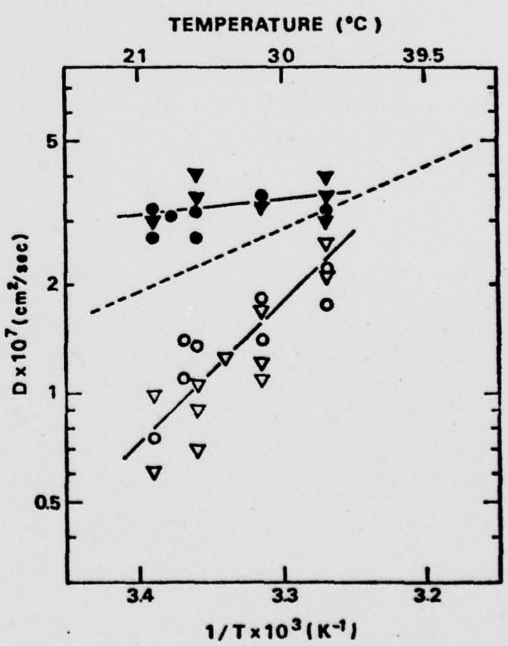

FIG. 4. Temperature dependences of $D_\parallel$ and $D_\perp$ in the nematic phase of MBBA. Upper line, $D_\parallel$, under homogeneous boundary conditions; ▾, no magnetic field applied; •, 10 kOe magnetic field applied parallel to the walls. Dotted line, D_0, extrapolated from experiments in isotropic phase. Bottom line, $D_\perp$, ▽, homeotropic boundary conditions utilizing both disc source and line source; ○, homogeneous boundary conditions with a 10 kOe magnetic field applied perpendicular to the direction of diffusion.

ciably alter the value of $D_\parallel$, the experiment was conducted with a 10 kOe magnetic field applied parallel to the molecular axis of MBBA. As long as the sample is in the magnetic field, no cholesteric texture is formed; i.e., one is above the critical field for the cholesteric–nematic transition. As soon as the field is removed, the Grandjean pattern develops and $D_\parallel$ can be evaluated. It can be seen in Fig. 4 that the magnetic field has little or no effect on $D_\parallel$.

It is also possible to determine $D_\perp$ in a similar manner using a 10 kOe field. In this case, the field is again applied parallel to the glass walls and parallel to the uniaxially aligned MBBA molecules, but the diffusant enters the sample perpendicular to the molecular axis of MBBA. These data are also given in Fig. 4 and compared with values of $D_\perp$ determined from the totally different boundary conditions discussed below.

Diffusion into homeotropically aligned nematic

Two boundary conditions were employed in these experiments. In the first, a semi-infinite line source of CMV was allowed to diffuse into homeotropically aligned MBBA, a configuration in which $D_\perp$ is determined. The appropriate equation for this boundary condition is the same as given in Eq. (2) above. The average pitch is measured from a group of fingerprints such as those shown in Fig. 2; the concentration is taken from the experimentally determined pitch–concentration relationship shown in Fig. 3. Typical data for $\ln C$ vs (penetration depth)^2 are given in Fig. 5. Values for $D_\perp$ as a function of temperature are plotted in Fig. 4 and compared with the determination of $D_\perp$ in a magnetic field visualized under homogeneous boundary conditions.

$D_\perp$ was also determined under homeotropic alignment using a circular disc source diffusant. When the diffusant is initially distributed uniformly in a circular disc of radius a and allowed to diffuse into an infinite plane surface, the concentration C at radius r and time t is given by[30]

$$C = a\,C_0 \int_0^\infty J_1(ua)\,J_0(ur)\,e^{-Dtu^2}\,du\,, \tag{6}$$

where C_0 is the initial concentration in the region $0 < r < a$. J_0 and J_1 are Bessel functions of the first kind and of order 0 and 1, respectively. A computer program was used to give the best value of $D_\perp$ from sets of measurements of C and r. Values of $D_\perp$ determined in this manner are plotted in Figs. 4 and 6 and agree well with $D_\perp$ as determined by the other two methods.

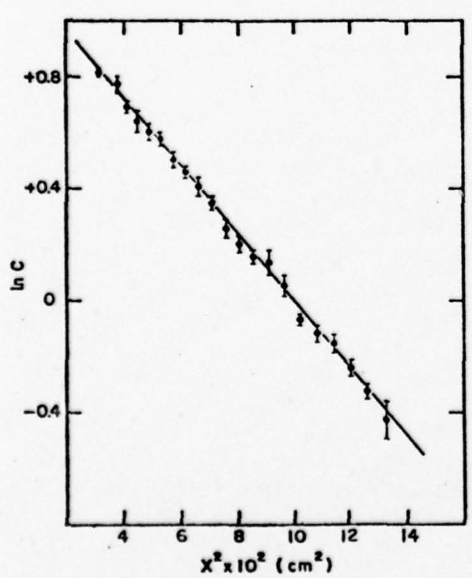

FIG. 5. ln concentration (weight %) vs (penetration depth)^2 as determined from the fingerprint pattern at 26.5° for CMV diffusing into MBBA. Sample thickness is 12.7 μm.

Diffusion in the isotropic phase

When the walls of the diffusion cell are treated with lecithin or silicon monoxide and the sample is heated above the isotropic transition temperature of MBBA, experiments may be conducted to determine D_0, the isotropic diffusion coefficient, in the following manner: after the diffusion anneal in the isotropic phase, the sample is quenched to room temperature. The sample develops either the fingerprint or Grandjean texture, depending on the wall treatment, and the diffusion coefficient is evaluated in the appropriate manner. Data obtained in this way, using two boundary conditions, are presented in Fig. 6 together with the nematic phase diffusion data. No data can be obtained very close to the isotropic transition temperature, which is suppressed several degrees in the presence of the cholesteric diffusant.

DISCUSSION

By taking advantage of strong wall coupling to provide orientation and textural changes to provide visualization of the concentration gradient, a simple method has been developed to study diffusion in nematic phases. In the initial system studied, a cholesteryl ester (CMV) was chosen as the diffusant, and it is obvious that comparison with other data requires correcting for the mass discrepancies, particularly with the relatively high diffusant concentrations required in this method.

One normally expects diffusivities of impurities to equal that of the solvent when the size of the impurity is comparable to or smaller than the solvent molecules.[32] Since $D \sim m^{-1/2}$, data with large diffusants can be used to estimate self-diffusion coefficients by correcting the data by the approximation[13]

$$\frac{D_{\text{solvent}}}{D_{\text{impurity}}} = \left(\frac{m_{\text{impurity}}}{m_{\text{solvent}}}\right)^{1/2}. \tag{7}$$

Table I compares data selected from Figs. 4 and 6 with earlier work on diffusion in MBBA. For the self-diffusion coefficient $D_\parallel$ at ~25°, NMR data by Blinc *et al.*[23] give a value of $2 \pm 1 \times 10^{-6}$; Murphy and Doane,[22] employing the solute molecule tetramethylsilane in a pulsed NMR study, obtained a value of 1×10^{-6}, which can be corrected for the mass discrepancy to give 0.6×10^{-6} for the self-diffusion coefficient. Correcting the data in this work for the mass of CMV gives 0.4×10^{-6} for the self-diffusion coefficient of MBBA. Other comparisons for

TABLE I. Values of diffusion coefficients for MBBA.

Method	Reference	Temp. °C	$D_{exp}\times 10^6$ cm^2 sec^{-1} D_0	$D_\parallel$	$D_\perp$	$D_{self}\times 10^6$ cm^2 sec^{-1} D_0	$D_\parallel$	$D_\perp$	E_a kcal mole^{-1}
NMR	23	21.0	···	2.0	···	···	2.0	···	···
NMR	22	43.0	1.0	···	···	1.0	···	···	6
NMR impurity	19	25.0	···	1.0	···	···	0.6	···	···
Tritium tracer	12	25.0	···	>0.5	0.35	···	>0.5	0.35	···
Optical	this work	24.5	···	0.3	···	···	0.4	···	~1
Optical	this work	24.5	···	···	0.1	···	···	0.13	17±2.5
Optical	this work	44.0	0.5	···	···	0.6	···	···	8±1.6

data on D_0 and $D_\perp$ are given in Table I.

In general, our values for D tend to be lower than those reported in other studies; the liquid crystal layers are very well oriented and strongly wall coupled, and these factors, in addition to the problem of properly correcting for the mass discrepancy in the diffusant, may lead to the lower values. One would expect the diffusion anisotropy to be roughly the same as the inverse of the viscosity anisotropy since $D \sim \eta^{-1}$ from the Einstein equation. Using Martinoty and Candau's viscosity data,[1] $\eta_\perp/\eta_\parallel \sim 1.5$. $D_\parallel/D_\perp$ at 24.5° is ~3 in our work. In a preliminary experiment injecting CMV into uniaxially and homogeneously aligned MBBA in a 10 kOe magnetic field, we observed an elliptical diffusion pattern; the axial ratios of this ellipse imply that $D_\parallel/D_\perp \sim 1.5 \pm 0.2$. Considering the scatter in the present diffusivity data, it is not possible to resolve this problem at present.

The activation energy for the diffusion process in the isotropic phase of MBBA agrees fairly well with the value reported by Ghosh and Tettamanti.[22] No earlier data are available for the activation energies E_a of $D_\parallel$ and $D_\perp$ in MBBA, but one can estimate an E_a for $D_\perp$ of 7.3 kcal/mole^{-1} for p-azoxyanisole from Yun and Frederickson's data.[24] The present value for E_a of $D_\perp$ (17±2.5 kcal/mole^{-1}) seems more reasonable for a phase intermediate between a molecular solid, where typical values[33-36] of E_a are in the range 20–60 kcal mole^{-1}, and the isotropic E_a of ~8 kcal mole^{-1} for MBBA. Extrapolating the $D_\perp$ data of Fig. 4 to the melting point of MBBA, one would estimate $D_\perp$ to be $\sim 0.5\times 10^{-7}$ cm^2 sec^{-1}; Blinc *et al.*[23] estimate a value for D in solid MBBA, 1° below the melting point, as 0.2×10^{-7} cm^2 sec^{-1}.

It has been suggested[24] that the relationships between $D_\parallel$, $D_\perp$, and D_0, the diffusion coefficient in the disoriented liquid, is given by

$$D_0 = \tfrac{1}{3}(2D_\perp + D_\parallel) . \quad (8)$$

By extrapolating D_0 linearly from the isotropic phase, and calculating D_0 from the experimentally determined values of $D_\parallel$ and $D_\perp$, one has another check on the validity of the data. This comparison is given in Table II. The experimentally determined values estimate D_0 to be about 20% lower than the extrapolated values.

It is likely that this optical method of determining diffusion coefficients can provide useful data on a number of systems. For example, by employing an optically active nematic liquid crystal as the diffusant into the racemic form of the same material, one can approximate self-diffusion. Such a nematogenic system has recently been synthesized by Dolphin *et al.*[37] Because of the suppression of the melting point of MBBA by impurity diffusant, it was not possible to determine D close to the

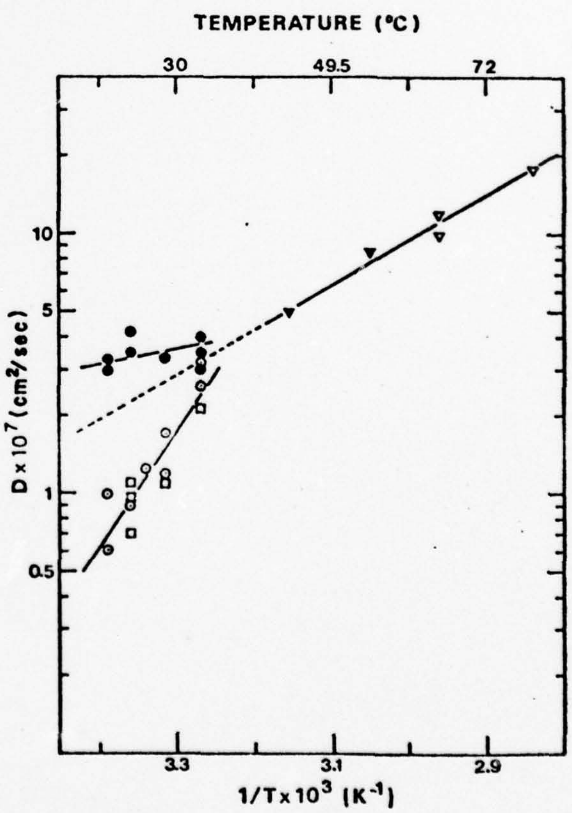

FIG. 6. Temperature dependences of $D_\parallel$, $D_\perp$, and D_0 in nematic and isotropic phases of MBBA. Isotropic phase: ▽, homeotropic alignment; ▾, homogeneous alignment. Nematic phase: upper curve, $D_\parallel$, homogeneous boundary conditions; lower curve, $D_\perp$, determined under homeotropic boundary conditions; ○, line source; □, disc source.

TABLE II. Comparison of D ($\times 10^7$ cm^2 sec^{-1}) extrapolated from isotropic phase and calculated from nematic phase.

T °C	$D_\perp$	$D_\parallel$	$D_0 = 1/3(2D_\perp + D_\parallel)$ calculated	D_0 extrapolated
33	2.2	3.5	2.7	3.2
28.5	1.5	3.4	2.2	2.7
24.5	1.0	3.3	1.8	2.2
22	0.8	3.0	1.6	2.0

nematic–isotropic transition where one might expect anomalies such as those observed in viscosity data.[1] It may be possible to obtain such data in the chiral nematic system just mentioned.

By aligning a cholesteric sample and allowing a nematogen to diffuse into it, D for a cholesteric system may be also measured; no measurements on cholesteric systems by other methods have as yet been successful.[24] The preliminary experiment described above on determining the anisotropy of diffusion by simply photographing the elliptical pattern formed when a cholesteric diffusant migrates into a uniaxially aligned nematic is also quite promising. After this work was completed, a communication appeared by Rondelez, in which diffusion anisotropies were measured and diffusion coefficients estimated by injecting dyes into uniaxially and homogeneously aligned MBBA in a magnetic field.[38] In our work, the elliptical pattern obtained when CMV was injected into MBBA gave $D_\parallel/D_\perp \sim 1.5$. Rondelez reports $D_\parallel/D_\perp \sim 1.6$ for two dyes diffusing into MBBA. He then attempts to estimate the diffusion coefficients $D_\parallel$ and $D_\perp$ by analyzing the optical density distribution in the ellipse with a densitometer. For the diffusion of methyl red, which is similar in size and shape to MBBA, $D_\parallel = 2.6 \pm 0.3\times10^{-7}$ cm^2 sec^{-1}, and $D_\perp = 1.6 \pm 0.3\times10^{-7}$ cm^2 sec^{-1} at 22°. Our determination of $D_\parallel$ agrees quite well with these values, but our direct determination of $D_\perp$ under several boundary conditions indicates it is probably smaller by a factor of 2. Further work on these systems is in progress.

ACKNOWLEDGMENT

The authors wish to thank Dr. R. Y. Lee of the Temple University Computer Activity for help with programming the calculations.

*This work was supported by the National Science Foundation under Grant No. GP-25988 and the U. S. Army Research Office under Grant No. DAHCO4-74-G-0186.

[1]See, for example, P. Martinoty and S. Candau, *Liquid Crystals* 3, *Part II*, edited by G. H. Brown and M. M. Labes (Gordon and Breach, London, 1972), p. 881. This paper relates viscosity coefficients to continuum theory as developed by J. L. Ericksen and F. M. Leslie.

[2]T. Svedberg, Kolloid-Z. 22, 68 (1918).

[3]T. Svedberg, Kolloid-Z. 18, 54, 101 (1916).

[4]T. Svedberg, Kolloid-Z. 21, 19 (1917).

[5]G. T. Stewart, Nature (Lond.) 183, 873 (1959).

[6]C. Robinson, Trans. Faraday Soc. 62, 571 (1956).

[7]M. M. Labes, Nature (Lond.) 211, 968 (1966).

[8]G. T. Stewart, Mol. Cryst. Liq. Cryst. 7, 75 (1969).

[9]K. D. Lawson and T. J. Flautt, J. Am. Chem. Soc. 89, 5489 (1967).

[10]For example, see E. F. Carr, Adv. Chem. Ser. 63, 76 (1967).

[11]G. Durand, L. Leger, F. Rondelez, and M. Veyssie, Phys. Rev. Lett. 22, 227 (1967); R. B. Meyer, Appl. Phys. Lett. 14, 208 (1969); T. M. Laronge, H. Baessler, and M. M. Labes, J. Chem. Phys. 51, 4186 (1969).

[12]I. Teucher, H. Baessler, and M. M. Labes, Nat. Phys. Sci. 229, 25 (1971).

[13]W. Franklin, *Liquid Crystals* 3, *Part II*, edited by G. H. Brown and M. M. Labes (Gordon and Breach, London, 1972), p. 1125; also in Mol. Cryst. Liq. Cryst. 14, 227 (1971).

[14]R. Blinc, V. Dimic, J. Pirs, M. Vilfan, and I. Zupancic, Mol. Cryst. Liq. Cryst. 14, 97 (1971).

[15]R. Blinc and V. Dimic, Phys. Lett. A 31, 531 (1970).

[16]J. A. Janik, J. M. Janik, K. Otnes, and T. Ristle, Mol. Cryst. Liq. Cryst. 15, 189 (1971).

[17]K. Otnes, R. Pynn, J. A. Janik, and J. M. Janik, Phys. Lett. A 38, 335 (1972).

[18]R. Blinc, D. L. Hogenboom, D. E. O'Reilly, and E. M. Peterson, Phys. Rev. Lett. 23, 969 (1969).

[19]J. A. Murphy and J. W. Doane, Mol. Cryst. Liq. Cryst. 13, 93 (1971); erratum in Mol. Cryst. Liq. Cryst. 15, No. 2, (1971).

[20]R. Y. Dong, W. F. Forbes, and M. M. Pintar, Solid State Commun. 9, 151 (1971).

[21]J. A. Murphy, J. W. Doane, Y. Y. Hsu, and D. L. Fishel, Mol. Cryst. Liq. Cryst. 22, 133 (1973).

[22]S. R. Ghosh and E. Tettamanti, Phys. Lett. A 34, 361 (1973).

[23]R. Blinc, J. Pirs, and I. Zupancic, Phys. Rev. Lett. 30, 546 (1973).

[24]C. K. Yun and A. G. Fredrickson, Mol. Cryst. Liq. Cryst. 12, 73 (1970).

[25]H. Hakemi and M. M. Labes, J. Chem. Phys. 58, 1318 (1973).

[26]J. L. Janning, Appl. Phys. Lett. 21, 173 (1972).

[27]See, for example, P. Kassubek, and G. Meier, *Liquid Crystals* 2, *Part II*, edited by G. H. Brown (Gordon and Breach, London, 1972), p. 753.

[28]H. Gruler and G. Meier, Mol. Cryst. Liq. Cryst. 16, 299 (1972).

[29]I. Rault and P. E. Cladis, Mol. Cryst. Liq. Cryst. 16, 1 (1971).

[30]J. Crank, *The Mathematics of Diffusion*, Oxford U. P., London, 1956), p. 11, 27–29.

[31]Another way of evaluating $D_\parallel$ from Eq. (4) is as follows: if one considers any three successive lines k, $k+1$, and $k+2$ at distances x_k, x_{k+1}, and x_{k+2}, and can eliminate the integer value k from Eq. (4) and obtain the equation $e^{-\alpha y} + e^{\beta y} = 2$. Here, α and β are the measured values $(x_k^2 - x_{k+1}^2)$ and $(x_{k+1}^2 - x_{k+2}^2)$, respectively, and $y = 1/4D_\parallel t$. By a simple computer program, values of $D_\parallel$ were obtained in this way and agreed well with the values obtained from the slope of the ln$k$ vs x_k^2 relationship.

[32]M. H. Cohen and D. Turnbull, J. Chem. Phys. 31, 1164 (1959).

[33]C. H. Lee, H. K. Kevorkian, P. J. Reucroft, and M. M. Labes, J. Chem. Phys. 42, 1406 (1965).

[34]A. R. McGhie, H. Blum, and M. M. Labes, J. Chem. Phys. 52, 6141 (1970).

[35]G. Burns and J. N. Sherwood, Mol. Cryst. Liq. Cryst. 18, 91 (1972).

[36]E. Hampton, N. C. Lockhart, and J. N. Sherwood, Chem. Phys. Lett. 21, 191 (1973).

[37]D. Dolphin, Z. Muljiani, J. Cheng, and R. B. Meyer, J. Chem. Phys. 58, 413 (1973).

[38]F. Rondelez, Solid State Commun. 14, 815 (1974).

Pitch-concentration relationships in multicomponent liquid crystal mixtures*

C. S. Bak and M. M. Labes

Department of Chemistry, Temple University, Philadelphia, Pennsylvania 19122
(Received 24 December 1974)

The variation of helical pitch in multicomponent liquid crystal mixtures is derived using the concept of the long-range distortions induced by chiral molecules in a nematic matrix. The pitch in a mixture is a quadratic function of the number densities of component molecules of given molecular twisting powers. The pitch variation becomes a linear function of number densities only when the twisting powers satisfy certain special conditions. The nonlinear pitch relation formulated herein is shown to describe typical experimental data on nematic-cholesteric mixtures and allows determination of experimental values of the molecular twisting power.

INTRODUCTION

It has long been known that when a cholesteric liquid crystal is added to a nematic compound, or when cholesteric compounds are mixed, the resultant pitch depends on concentration factors, but the precise nature of the pitch-concentration relationship has been difficult to define. At very low concentrations of a cholesteric (chiral) additive to a nematic liquid, pitch has been found experimentally to be inversely proportional to concentration.[1] By extending the theory of Maier and Saupe,[2] the dispersion interaction energy between two molecules in adjacent planes with a finite twist angle has been calculated by Goossens[3] considering both dipole-dipole and dipole-quadrupole terms and predicting a linear relationship between pitch^{-1} and concentration. de Gennes[4] has presented a treatment of the problem which considers the distortions created in a nematic liquid by a floating (chiral) object which also predicts a linear relationship.

For many cholesteric binary mixtures of A and B, the observed pitch p has been found to be *almost* equal to the weight average of each component following the linear additivity rule[5,6]

$$1/p = w_A/p_A + w_B/p_B , \tag{1}$$

where p_A and w_A are the pitch and the weight fraction of A component, etc. There are, however, several examples[7] where the measured pitch in the mixture deviates considerably from Eq. (1). It has been shown that Eq. (1) fits experimental data more closely when w_A is the weight fraction rather than the mole fraction; nevertheless, the pitch variation over the entire range of weight fraction is clearly incompatible with Eq. (1). Similarly for a binary mixture of cholesteric and nematic compounds, although the relation pw_A = constant holds for small weight fraction w_A, considerable discrepancies have also been observed when the cholesteric concentrations were high.[7,8]

In this work a pitch-concentration relationship is derived which accurately describes the relationship in multicomponent liquid crystal mixtures; the relationship is employed to analyze some of the available experimental data. The relationship is derived by extending de Gennes' concept of long range distortions induced by chiral molecules in a nematic matrix[4] to the general case of cholesteric-cholesteric mixtures. The basic parameters that determine the pitch of a mixture are the intermolecular twisting powers and the number densities of component molecules. Unlike Eq. (1), the general form of pitch relation in the mixture is quadratic in the number density but can be reduced to the linearly additive Eq. (1) when the intermolecular twisting powers satisfy certain conditions. Analysis of experimental data on several binary mixtures of cholesteric and nematic compounds shows that the nonlinear relationship herein derived fits the data very well over the entire range of concentration, and the results give the molecular twisting powers between various molecules with high accuracy.

THEORY

When chiral molecules are introduced into a nematic liquid, the induced distortions of the nematic director $\mathbf{n}_0$ have been calculated by de Gennes[4] for the case of low concentrations only. The new director $\mathbf{n}(\mathbf{r})$ is

$$\mathbf{n} = \mathbf{n}_0 + \delta\mathbf{n} . \tag{2}$$

The local rotation at a distance r from the chiral solute is described by the vector $\boldsymbol{\omega}$, defined as

$$\delta\mathbf{n} = \boldsymbol{\omega} \times \mathbf{n}_0 . \tag{3}$$

This perturbation gives rise to the twist of the nematic director and has the form[4]

$$\boldsymbol{\omega} = -\beta\nabla(1/r) . \tag{4}$$

Here r is the distance between the chiral molecule and the point of observation in the nematic matrix. The parameter β has the dimension of a surface (cm^2) and is dependent on the orientation of the chiral molecule and the interaction between the chiral and nematic molecules.

To generalize the effect of introduction of *any* concentration of chiral molecules, one should include the probability that the introduced chiral molecules occupy the point of observation, and extend Eq. (4) to the general case of cholesteric-cholesteric mixtures. For a two-component cholesteric mixture of A and B, the vector ω at the point of observation contributed by A molecules located at distance r_A will depend on whether the point of observation is occupied by A or B molecules. Since the probability of A(B) molecules to be found at the point

of observation is $[n_A/(n_A+n_B)][n_B/(n_A+n_B)]$, where $n_A(n_B)$ is the number of A(B) molecules per cm^3 in the mixture, the effective vector ω for an A molecule will be

$$\omega_A = -\beta_A \frac{n_A}{n_A+n_B} \nabla\left(\frac{1}{r_A}\right) - \beta_{AB} \frac{n_B}{n_A+n_B} \nabla\left(\frac{1}{r_A}\right) . \quad (5)$$

Similarly for a B molecule

$$\omega_B = -\beta_B \frac{n_B}{n_A+n_B} \nabla\left(\frac{1}{r_B}\right) - \beta_{AB} \frac{n_A}{n_A+n_B} \nabla\left(\frac{1}{r_B}\right) .$$

The total vector ω is the summed contribution from all A and B molecules:

$$\omega = \sum_A \omega_A + \sum_B \omega_B .$$

If we follow the same procedure used in Ref. (4)

$$\nabla \cdot \omega = \frac{4\pi}{n_A+n_B} \{ \beta_A n_A^2 + 2\beta_{AB} n_A n_B + \beta_B n_B^2 \} .$$

For $\omega = (0, 0, (2\pi/p)z)$,

$$\frac{1}{2p} = \frac{1}{n_A+n_B} \{ \beta_A n_A^2 + 2\beta_{AB} n_A n_B + \beta_B n_B^2 \} . \quad (6)$$

Equation (6) is the basic generalized equation for relating pitch and concentration. Aside from the total number density n_A+n_B, Eq. (6) is quadratic in the partial number density of the components. Several special cases can now be described.

(1) For a single component cholesteric compound ($\beta_A = \beta_{AB} = \beta_B$, $n_A + n_B = N_A$ = constant),

$$1/2p = \beta_A N_A . \quad (7)$$

β_A is the effective (or mean) molecular twisting power between A molecules only. When β_A is positive (negative), the helical structure is right (left) handed.

(2) For a nematic compound, $p=\infty$. Hence $\beta = 0$.

(3) For a racemic mixture, $\beta_A = -\beta_B$. Since $p=\infty$ when $n_A = n_B$, we get $\beta_{AB} = 0$ from Eq. (6).

(4) For the special case when $\beta_{AB} = \frac{1}{2}(\beta_A + \beta_B)$, Eq. (6) reduces to

$$1/2p = \beta_A n_A + \beta_B n_B .$$

This is a linearly additive equation of the partial number density.

(5) For a mixture of cholesteric structure A and nematic structure B ($\beta_B = 0$),

$$\frac{1}{2p} = \frac{1}{n_A+n_B} \{ \beta_A n_A^2 + 2\beta_{AB} n_A n_B \} . \quad (8)$$

(6) For a low concentration of a cholesteric solute ($n_A \ll n_B$)

$$1/2p \approx 2\beta_{AB} n_A . \quad (9)$$

This is the well-known equation that describes the observed pitch for low cholesteric concentrations in a nematic liquid.[1,9]

In addition to describing the behavior of binary mixtures, Eq. (6) can easily be extended to a mixture of multicomponent cholesteric compounds (n_i, $i = 1,2,3,\cdots$)

$$\frac{1}{2p} = \frac{1}{\sum_i n_i} \left\{ \sum_i \beta_i n_i^2 + 2 \sum_{i<j} \beta_{ij} n_i n_j \right\} . \quad (10)$$

For the case when all the $\beta_{ij} = \frac{1}{2}(\beta_i + \beta_j)$, the above equation becomes a linearly additive law

$$\frac{1}{2p} = \sum_i \beta_i n_i . \quad (11)$$

ANALYSIS OF EXPERIMENTAL DATA

To test this theory, we have analyzed experimental data on several binary cholesteric and nematic mixtures which have been reported to disobey the linear additivity rule. Since most experimental data have been reported previously using the mole or weight fraction of component, it is convenient to convert Eq. (8) into these terms. To simplify the analysis, we assume that the volume change upon mixing the components is negligibly small. Then in terms of mole fraction of the cholesteric component, Eq. (8) has the form

$$1/2pMm_A = (N\beta_A - 2N\beta_{AB}) m_A + 2N\beta_{AB} , \quad (12)$$

where $m_A = n_A/(n_A+n_B)$ = mole fraction of the cholesteric component A,

$$M = \left[\left(\frac{M_A}{d_A} - \frac{M_B}{d_B}\right) m_A + \frac{M_B}{d_B}\right]^{-1} = \text{molar density of the mixture} ,$$

$M_A(M_B)$ = molecular weight of A(B) component,

$d_A(d_B)$ = density (g/cm^3) of pure A(B) component,

N = Avogadro's number .

In terms of weight fraction of the cholesteric component

$$\frac{M_A + (M_B - M_A) w_A}{2pdw_A} = \left\{ N\beta_A \frac{M_B}{M_A} - 2N\beta_{AB} \right\} w_A + 2N\beta_{AB} \quad (13)$$

where w_A = weight fraction of the cholesteric component A,

$$d = \frac{d_B}{1 + (d_B/d_A - 1) w_A} = \text{density (g/cm}^3\text{) of the mixture.}$$

The form of Eq. (12) or (13) should yield plots which give linear relationships from which the parameters $N\beta_A$ and $N\beta_{AB}$ (hereafter called the molar twisting powers) can readily be determined by extrapolating the straight line to $m_A(w_A) = 0$ and 1.

The experimental data analyzed below are the measured pitch–concentration relationships of several cholesteric-nematic mixtures. The compounds and references are as follows:

1. *N*-(*p*-methoxybenzylidene)-*p*-*n*-butylaniline (MBBA) + cholesteryl chloride (CC),[10]

2. MBBA + cholesteryl-2-(2-ethoxyethoxy) ethyl carbonate (CEEC),[11]

3. *p*-[*N*-(*p*-methoxybenzylidene) amino]-phenyl acetate (MBA) + cholesteryl propionate (CP),[8]

4. MBBA + cholesteryl oleyl carbonate (COC).[6]

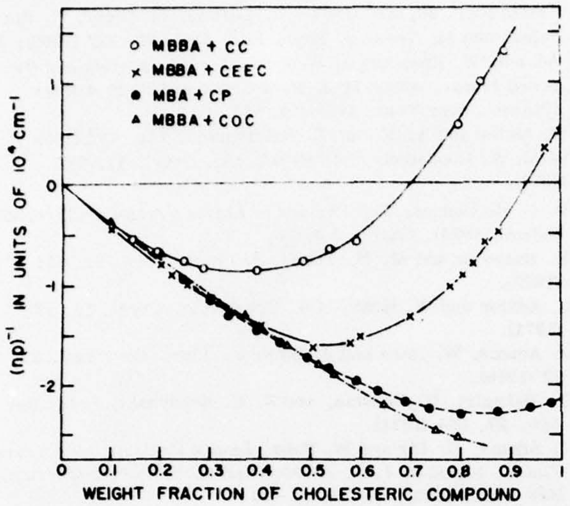

FIG. 1. Reciprocal pitch of binary nematic–cholesteric mixtures vs weight fraction of cholesteric compound.

Figure 1 is a plot of $(np)^{-1}$ vs the weight fraction of cholesteric compound for all the above binary systems. Here n denotes the mean index of refraction. When the helical sense of the mixture is left handed, the pitch is taken as negative.

In Fig. 2 all the data from Fig. 1 are plotted using Eq. (13). Approximate values of $n = 1.5$ and $d = 0.9$ g/cm^3 were taken for all the mixtures. By extrapolating the straight lines in Fig. 2 to $w_A = 0$ and 1, the molar twisting powers were obtained.

Table I is the summary of the molar twisting powers obtained in this manner. The overall uncertainty in the determination of the twisting powers if about 5%.

DISCUSSION

In Fig. 2 the data for each binary mixture fall on a straight line as predicted from Eq. (13), and indicate that the pitch–concentration relationship employed is satisfactory in explaining pitch variation of a wide variety of binary mixtures over the entire range of concentration. As discussed in the section on Theory, the pitch in a mixture is a quadratic function of the number density of components and it becomes a linear equation only when the intermolecular twisting powers satisfy the conditions $\beta_{ij} = \frac{1}{2}(\beta_i + \beta_j)$. If one uses other variables, such as mole fraction or weight fraction, the linearity of the equation can be altered. To illustrate this, let us consider Eqs. (12) and (13), and assume $d_A \approx d_B$ for simplicity. From Eq. (12) we see that pm_A = constant for the whole range of m_A if

$$M_A/M_B = N\beta_A/2N\beta_{AB} \, . \tag{14}$$

From Eq. (13), pw_A = constant if

$$N\beta_A/2N\beta_{AB} = 1 \, . \tag{15}$$

Thus the conditions for the linear additivity rule are different when considering mole or weight fraction. Consequently the pitch variation will be closer to the linear

TABLE I. The molar twisting powers in units of 10^6 cm^2 obtained from Fig. 2. The numbers in the parentheses are the molecular weight of the components.

Cholesteric (A) compound	$N\beta_A$ 10^6 cm^2	$N\beta_{AB}$ 10^6 cm^2 MBBA (267)	MBA (269)
CC(405)	+9.4	−7.6	
CP(443)	−8.2		−8.0
CEEC(547)	+2.7	−10.8	
COC(681)	−16.0	−10.7	

equation depending upon how closely the material parameters satisfy conditions (14) and (15). For example, in the mixture of MBBA + COC in Table I, $M_A/M_B - N\beta_A/2N\beta_{AB} = 1.80$ and $1 - N\beta_A/2N\beta_{AB} = 0.25$. This explains why Adams and Haas[6] observed the pitch–concentration variation being closer to linear behavior when plotted vs weight fraction than vs mole fraction. There is, however, no general rule that weight fractions necessarily give closer linearity than mole fractions.

It is interesting to note from Table I that the twisting power between different molecules ($N\beta_{AB}$) is far from being the average of the twisting powers of each molecule ($\frac{1}{2}N\beta_A$, since $\beta_B = 0$). In fact, the $N\beta_A$'s of the cholesteric compounds with carbonate groups (CEEC and COC) are considerably different and opposite in sign, while in MBBA the values of $N\beta_{AB}$ are similar and both negative. Even in the different nematic compounds (MBBA and MBA), dissolving CC and CP, which have opposite handedness, results in similar negative values of $N\beta_{AB}$.

The term $M_A + (M_B - M_A)w_A$ in the left hand side of Eq. (13) is important to include in calculations; without this term the data cannot be fit to a linear function. This confirms our assertion that the number densities of components are the basic parameters in determining the pitch of a mixture; the variation in number density for

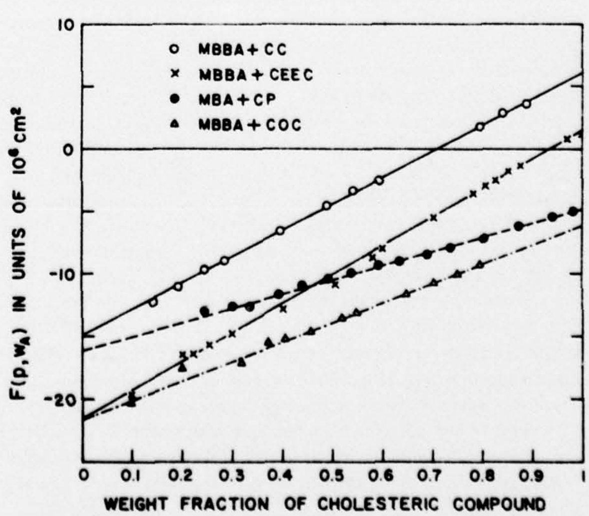

FIG. 2. Test of the validity of Eq. (13) by plotting $F(p, w_A) = [M_A + (M_B - M_A)w_A]/2pdw_A$ vs weight fraction of cholesteric compound in binary nematic–cholesteric mixtures.

different concentrations must be taken into account, particularly if the molecular weights of the components are significantly different.

Recently another attempt has been made to account for pitch–concentration relationships over an extended concentration range. Expanding Goossens' treatment[3] of dipolar and quadrupolar interactions between molecular layers, Finkelmann and Stegemeyer[12] have introduced quadratic terms into the equations and successfully account for nonlinearities. The parameters involved in their treatment are related to molecular polarizabilities and are not as readily accessible as the density-related parameters employed in this work.

In conclusion, the pitch–concentration relationship for liquid crystal mixtures formulated in this work agrees with experimental data on the nematic–cholesteric mixtures, and provides important materials parameters for the molecular twisting power. A further test of the theory in analyzing cholesteric–cholesteric mixtures and general multicomponent mixtures is in progress.

*This work was supported by the U. S. Army Research Office (Durham) under Grant No. DAHCO4-G-74-0186.

[1]R. Cano and P. Chatelain, C. R. Acad. Sci. B **253**, 1815 (1961); **259**, 252 (1964); R. Cano, Bull. Soc. Fr. Mineral. Cristallogr. **90**, 333 (1967); G. Durand, L. Leger, F. Rondelez, and M. Veyssie, Phys. Rev. Lett. **22**, 227 (1969); J. Adams, W. Haas and J. Wysocki, *Liquid Crystals and Ordered Fluids*, edited by J. F. Johnson and R. S. Porter (Plenum, New York, 1970), p. 463.

[2]W. Maier and A. Saupe, Z. Naturforsch. **14a**, 882 (1959).

[3]W. J. A. Goossens, Mol. Cryst. Liq. Cryst. **12**, 237 (1971).

[4]P. G. de Gennes, *The Physics of Liquid Crystals* (Clarendon, Oxford, 1974), Chaps. 3 and 6.

[5]H. Baessler and M. M. Labes, J. Chem. Phys. **52**, 631 (1970).

[6]J. Adams and W. Haas, Mol. Cryst. Liq. Cryst. **15**, 27 (1971).

[7]J. Adams, W. Haas and J. Wysocki, Phys. Rev. Lett. **22**, 92 (1969).

[8]T. Nakagiri, H. Kodama, and K. K. Kobayashi, Phys. Rev. Lett. **27**, 564 (1971).

[9]J. Adams, G. Dir and W. Haas, *Liquid Crystals and Ordered Fluids*, edited by J. F. Johnson and R. S. Porter (Plenum, New York, 1974), Vol. 2, p. 42.

[10]F. D. Saeva and J. Wysocki, J. Am. Chem. Soc. **93**, 5928 (1971).

[11]N. Oron, K. Ko, L. J. Yu, and M. M. Labes, *Liquid Crystals and Ordered Fluids*, edited by J. F. Johnson and R. S. Porter (Plenum, New York, 1974), Vol. 2, p. 403.

[12]H. Finkelmann and H. Stegemeyer, Ber. Bunsenges. Phys. Chem. **78**, 869 (1974); H. Stegemeyer, Ber. Bunsenges. Phys. Chem. 78, 860 (1974).

Analysis of pitch–concentration dependences in some binary and ternary liquid crystal mixtures*

C. S. Bak and M. M. Labes

Department of Chemistry, Temple University, Philadelphia, Pennsylvania 19122
(Received 27 February 1975)

Utilizing a general equation in which pitch in a mixture of liquid crystals is a quadratic function of the number densities of component molecules of given molecular twisting powers, we treat two special cases: binary cholesteric mixtures and a ternary mixture of two cholesteric and one nematic compounds. Experimental data are shown to be adequately described by the equation over the entire concentration range.

INTRODUCTION

Recently we have shown[1] that a generalized pitch–concentration relationship in multicomponent liquid crystal mixtures can be derived from de Gennes' concept[2] of long range distortions induced by chiral molecules in a nematic matrix. When the effective distortions caused by chiral molecules are properly calculated allowing the matrix itself to be chiral, the resultant pitch in the mixture is found to be, in general, a quadratic function of the number densities of component molecules. This quadratic pitch relation becomes a linear equation of number densities when the intermolecular twisting powers satisfy certain conditions.

The twist between cholesteric layers has also been calculated by Goossens[3] from considerations of dipole–dipole and dipole–quadrupole interactions between molecules. Recently Stegemeyer[4] has extended Goossens' treatment to the case of binary mixtures, and derived a pitch–concentration relation for binary systems.[4,5] Although the pitch variation derived in our recent work[1] is based on the concept of long range distortions, and contains fewer material parameters than the equation derived by Stegemeyer,[4] our equations describe accurately the observed pitch variation in many nematic–cholesteric mixtures, and can easily be extended to the general case of arbitrary multicomponent mixtures.[1] In the present work, the validity of this pitch–concentration relation has been tested for binary cholesteric mixtures as well as a ternary mixture consisting of two cholesteric and one nematic compounds. Analyses of available experimental data show that the theoretical pitch relation fits the data closely over the whole range of concentration; molecular twisting powers between various liquid crystals can also be calculated and show interesting differences for data on different pairs of molecules.

THEORY

The helical pitch p of a multicomponent liquid crystal mixture is given by[1]

$$1/2p=\left(1\Big/\sum_i n_i\right)\left\{\sum_i \beta_i n_i^2+2\sum_{i<j}\beta_{ij}n_in_j\right\}, \tag{1}$$

where n_i ($i=1,2,3\ldots$) is the partial number density of ith component molecules in the mixture. The molecular twisting powers β's are defined in Ref. 1 and have the dimension of a surface (cm^2). To analyze the experimental data on binary and ternary mixtures, Eq. (1) can be treated as follows:

(1) For a binary mixture of cholesteric A and cholesteric B components, Eq. (1) becomes

$$1/2p=[1/(n_A+n_B)]\{\beta_A n_A^2+\beta_B n_B^2+2\beta_{AB}n_An_B\}. \tag{2}$$

Since most available experimental data on the measured pitch in mixtures have been reported using the mole or weight fraction of component, it is convenient to convert Eq. (2) to these terms. To simplify the data analysis, the volume change upon mixing the components is assumed to be negligibly small. In terms of mole fraction, Eq. (2) has the form

$$1/2pM=N\{\beta_A m_A^2+\beta_B(1-m_A)^2+2\beta_{AB}m_A(1-m_A)\}, \tag{3}$$

where $m_A=n_A/(n_A+n_B)$ is the mole fraction of the cholesteric component A, $M=[(M_A/d_A-M_B/d_B)m_A+M_B/d_B]^{-1}$ is the molar density of the mixture, $M_A(M_B)$ is the molecular weight of A(B) component, $d_A(d_B)$ is the density (g/cm^3) of pure A(B) component, and N is Avogadro's number. Introducing a new parameter $\delta\beta_{AB}$, defined as

$$2\beta_{AB}\equiv\beta_A+\beta_B+\delta\beta_{AB}, \tag{4}$$

Eq. (3) can be written

$$1/2pM=N\{(\beta_A-\beta_B)m_A+\beta_B+\delta\beta_{AB}m_A(1-m_A)\}. \tag{5}$$

Here the new parameter $\delta\beta_{AB}$ is a measure of the deviation of β_{AB} from the mean value of β_A and β_B, but it does not necessarily imply that $\delta\beta_{AB}$ is generally close to zero. In fact, as shown in Ref. 1, β_{AB} is far from being the mean value of β_A and β_B for many liquid crystals. Here Eq. (5) is merely a convenient form for data analysis because, by adjusting the value of $\delta\beta_{AB}$, a plot of $1/2pM-N\delta\beta_{AB}m_A(1-m_A)$ vs m_A should show linear behavior, and the parameters β_A and β_B can be obtained at $m_A=1$ and 0.

In terms of weight fraction, Eq. (2) can be written

$$\frac{M_A+(M_B-M_A)w_A}{2pd}=N\left\{\frac{M_B}{M_A}\beta_A w_A^2+\frac{M_A}{M_B}\beta_B(1-w_A)^2+2\beta_{AB}w_A(1-w_A)\right\}, \tag{6}$$

where w_A = weight fraction of the cholesteric component A;

$$d=\frac{d_B}{1+(d_B/d_A-1)w_A}$$

is the density (g/cm^3) of the mixture. By introducing a new parameter $\Delta\beta_{AB}$, defined as

$$2\beta_{AB}\equiv(M_B/M_A)\beta_A+(M_A/M_B)\beta_B+\Delta\beta_{AB}, \tag{7}$$

Eq. (6) has the form

$$\frac{M_A+(M_B-M_A)w_A}{2pd}$$

$$=N\left\{\left(\frac{M_B}{M_A}\beta_A-\frac{M_A}{M_B}\beta_B\right)w_A+\frac{M_A}{M_B}\beta_B+\Delta\beta_{AB}w_A(1-w_A)\right\}. \quad (8)$$

After adjusting $\Delta\beta_{AB}$, the plot of $[M_A+(M_B-M_A)w_A]/2pd - N\Delta\beta_{AB}w_A(1-w_A)$ vs w_A should also be linear, and the parameters β_A and β_B will be obtained at $w_A=1$ and 0.

(2) For a ternary mixture consisting of two cholesteric (A and B) and one nematic (C) compounds, Eq. (1) becomes ($\beta_C=0$)

$$\frac{1}{2p}=\frac{1}{n_A+n_B+n_C}\times\{\beta_A n_A^2+\beta_B n_B^2+2\beta_{AB}n_An_B+2\beta_{AC}n_An_C+2\beta_{BC}n_Bn_C\}. \quad (9)$$

The helical pitch measured in this type of ternary mixture has been reported by Adams, Dir, and Haas.[6] The composition variables they used to represent a mixture are the weight fraction of only one cholesteric component A in a mixture of two cholesteric compounds A and B, and the weight fraction of nematic component C in the total mixture of A, B, and C. When Eq. (9) is converted to these variables, assuming that the volume change upon preparing the mixture is negligible and that all the densities of the components are the same, one obtains

$$\frac{1}{2pd}=N\left\{\frac{\beta_A}{M_A}\alpha(1-w_C)+\frac{\beta_B}{M_B}(1-\alpha)(1-w_C)\right\}+NM'\left\{\frac{\delta\beta_{AB}}{M_AM_B}\alpha(1-\alpha)(1-w_C)^2+\frac{\delta\beta_{AC}}{M_AM_C}\alpha w_C(1-w_C)+\frac{\delta\beta_{BC}}{M_BM_C}(1-\alpha)w_C(1-w_C)\right\}, \quad (10)$$

where α is the weight fraction of A component in the mixture of A and B only, w_C is the weight fraction of C component in the total mixture of A, B, and C compounds,

$$2\beta_{AB}=\beta_A+\beta_B+\delta\beta_{AB},$$

$$2\beta_{AC}=\beta_A+\delta\beta_{AC},\ \text{etc.},$$

$$M'^{-1}=\frac{\alpha(1-w_C)}{M_A}+\frac{(1-\alpha)(1-w_C)}{M_A}+\frac{w_C}{M_C}.$$

For the special case when $\delta\beta_{AB}=0$ and $M'=$ constant, Eq. (10) is identical to the empirical equation Adams *et al.*[6] introduced to explain the pitch variation in this type of ternary system. Equation (10) can be rearranged in the form

$$\frac{1}{2pdM'(1-w_C)}=N\left\{\frac{\beta_A}{M_A}\alpha+\frac{\beta_B}{M_B}(1-\alpha)\right\}M'^{-1}+N\left\{\frac{\delta\beta_{AB}}{M_AM_B}\alpha(1-\alpha)(1-w_C)+\frac{\delta\beta_{AC}}{M_AM_C}\alpha w_C+\frac{\delta\beta_{BC}}{M_BM_C}(1-\alpha)w_C\right\}. \quad (11)$$

The right-hand side of Eq. (11) is linear in w_C. Thus a plot of the left-hand side of Eq. (11) vs w_C for a fixed α value should yield linear behavior over the entire composition range of w_C.

ANALYSIS OF EXPERIMENTAL DATA

A. Binary cholesteric mixtures

Below is an analysis of data for binary cholesteric mixtures reported by Finkelmann and Stegemeyer.[5] The mixtures they studied are three sets of a binary system made with all the possible pairs of three cholesteric compounds: cholesteryl chloride (CC), cholesteryl-2-(2-ethoxyethoxy) ethyl carbonate (CEEC), and p-(4-cyanobenzalamino)-cinnamic acid active amyl ester (CBAC). Since the prepared mixtures are represented in terms of mole fraction of one cholesteric component, Eq. (5) will be employed to analyze the data. Figure 1 is the plot of $(2pM)^{-1}$ vs mole fraction m_A for all three sets of binary mixtures.[7] An approximate index of refraction $n=1.5$ and density $d=0.9$ g/cm³ were used for all the compounds.

For CBAC + CC and CBAC + CEEC, the strong downward curvature in Fig. 1 indicates that, even though the pure component is a right-handed cholesteric compound, the twisting power between different molecules is left-handed, and consequently reduces the reciprocal pitch when they are mixed. In particular, the twisting power between CBAC and CEEC molecules is so strongly left-

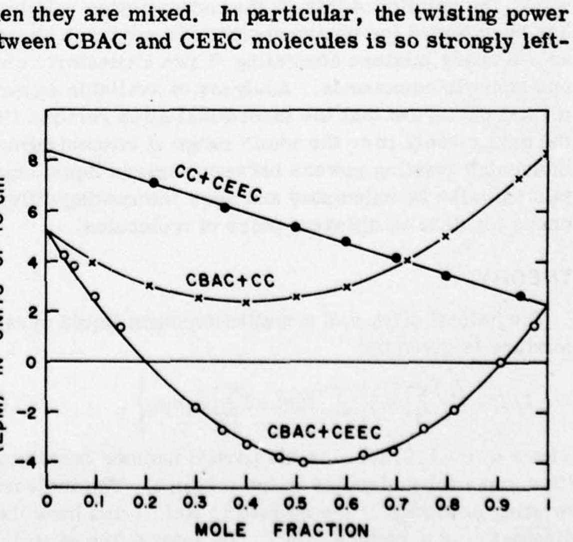

FIG. 1. Plot of $(2pM)^{-1}$ vs mole fraction of CEEC in CC (●); CC in CBAC (×); CEEC in CBAC (○). The notation is given in Eqs. (3)–(5). The data are taken from Ref. 5.

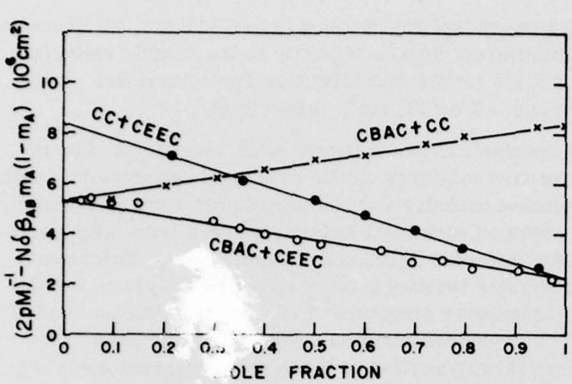

FIG. 2. Test of the validity of Eq. (5) by replotting the data of Fig. 1 for $(2pM)^{-1} - N\delta\beta_{AB}m_A(1-m_A)$ vs mole fraction of CEEC in CC (●); CC in CBAC (×); CEEC in CBAC (○). The notation is given in Eqs. (3)–(5). The parameter values are given in Table I.

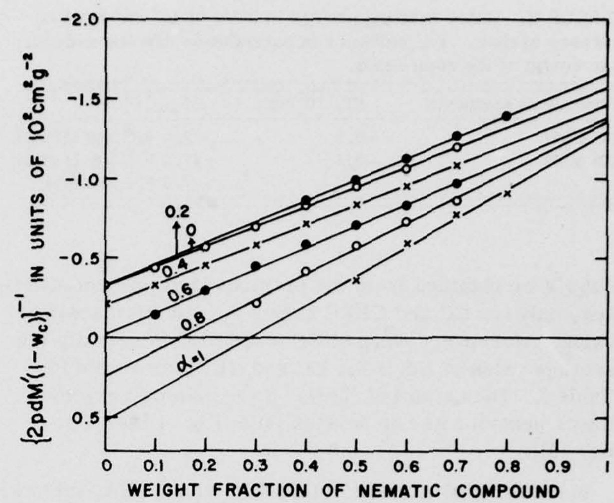

FIG. 3. Plot of $\{2pdM'(1-w_C)\}^{-1}$ vs weight fraction of nematic compound. The notation is given in Eqs. (10) and (11). The data are taken from Ref. 6.

handed that the resultant pitch of certain mixtures is completely reversed to a left-handed structure, as indicated by the negative value of $(2pM)^{-1}$ in Fig. 1. In Fig. 2, $(2pM)^{-1} - N\delta\beta_{AB}m_A(1-m_A)$ is plotted vs m_A [see Eq. (5)] after the value $\delta\beta_{AB}$ is adjusted so that each set of data points for a given binary system falls on a straight line. Here care was taken to have straight lines meet at the same point representing a value for the pure compound. The other two parameters β_A and β_B were subsequently obtained from the straight lines extrapolated to $m_A = 1$ and 0. The molar twisting powers $N\beta$'s obtained in this manner are summarized in Table I.

B. Ternary mixture

Experimental data reported by Adams, Dir, and Haas[6] for a ternary mixture will now be analyzed. The system consists of cholesteryl chloride (CC), cholesteryl nonanoate (CN) and N-(p-methoxybenzylidene)-p-n-butylaniline (MBBA). As mentioned in the section on theory, the right hand side of Eq. (11) is linear in w_C (the weight fraction of nematic compound). A plot of the left hand side of Eq. (11) vs w_C for a few fixed α values is shown in Fig. 3, which clearly indicates that each set of data points for a given α falls on a straight line. One can also note from Eq. (11) that when $\omega_c = 1$, the right hand side of Eq. (11) is again linear in α. The values of the left hand side of Eq. (11) extrapolated to $w_C = 1$ are obtained from Fig. 3 and plotted in Fig. 4 for various α values. The molecular twisting powers obtained with Eq. (11) for this ternary system are summarized in Table II where the accuracy is generally about 5%. Only the parameter β_{AB} (the twisting power between CC and CN molecules) is much less accurate in value (about 20%) as compared to the other obtained parameters. This low accuracy appears to be due to the factor $\alpha(1-\alpha)(1-w_C)$ in Eq. (11); this factor can change only between 0 and 0.25 over the entire composition range, whereas the factors in the other terms in Eq. (11) can change from 0 to 1.

TABLE I. Molar twisting powers in units of 10^6 cm^2 obtained from Fig. 2. The numbers in parentheses are the molecular weight of the compounds.

Cholesteric compound	$N\beta_A$ 10^6cm^2	$N\beta_{AB}$ 10^6cm^2
CC (405)	+8.4	−1.9 (CBAC and CC)
CEEC (547)	+2.2	+5.4 (CC and CEEC)
CBAC (346)	+5.3	−11.4 (CBAC and CEEC).

DISCUSSION

The pitch variation shown in Fig. 1 for three binary cholesteric mixtures becomes linear in Fig. 2 when the pitch is corrected with an adjusted value of $\delta\beta_{AB}$ according to Eq. (5). This indicates that the pitch–concentration relationship formulated in Eq. (5) is satisfactory in explaining the observed pitch variation in a wide variety of binary cholesteric mixtures over the entire concentration range. It is interesting to note from Table I that the molar twisting powers $N\beta_A$'s for three pure cholesteric compounds are all positive, while the twisting powers $N\beta_{AB}$'s between different molecules vary widely from positive to negative values. In fact, among all the

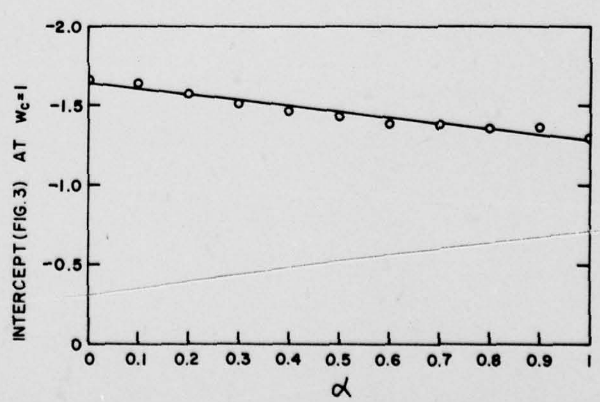

FIG. 4. Extrapolated values of $\{2pdM'(1-w_C)\}^{-1}$ to $w_C = 1$ obtained from Fig. 3 are plotted for various α values. The notation is given in Eqs. (10) and (11).

TABLE II. Molar twisting powers in units of $10^6 cm^2$ for the ternary system. The numbers in parentheses are the molecular weight of the compounds.

Cholesteric compound	$N\beta_A$ $10^6 cm^2$	$N\beta_{AB}$ $10^6 cm^2$
CC (405)	+9.1	−7.0 (CC and MBBA)
CN (527)	−9.2	−11.5 (CN and MBBA)
		~−7.0 (CC and CN)

$N\beta_{AB}$'s we obtained from the previous[1] and present analyses, only for CC and CEEC does $N\beta_{AB}$ exhibit a positive value. Moreover, $N\beta_{AB}$ of CC and CEEC is actually the average value of $N\beta_A$'s for CC and CEEC as shown in Table I. Thus a plot of $(2pM)^{-1}$ vs m_A shows very good linear behavior as can be seen from Fig. 1 [see also Eq. (5)].

In the ternary mixture of CC, CN, and MBBA, Adams *et al.*[6] analyzed the measured pitch using an empirically introduced pitch–concentration relation. Their relation is identical to the special case of Eq. (10) when M' = constant and $\delta\beta_{AB} = 0$. Adams *et al.*[6] found that their pitch relation fit data over a substantial composition range, but it would not fit over the entire range. For this ternary mixture of CC, CN, and MBBA, M' is not a constant but can vary by a factor of 2 over the composition range. Moreover, our data analysis in this ternary system indicates that $\delta\beta_{AB}$ *must* be *nonzero* to be able to explain successfully the pitch variation over the entire composition range using Eq. (10) [and Eq. (11)].

The $N\beta_A$'s of CC in Tables I and II (8.4 and 9.1×10^6 cm^2) compare favorably with 9.4×10^6 cm^2 obtained in previous work.[1] The small discrepancy (about 10%) for each independent data source is, we believe, attributable to the different degree of purity in the sample materials. The $N\beta_{AB}$'s for CC and MBBA in Table I and Ref. 1 are -7.0 and -7.6×10^6 cm^2, respectively.

In conclusion, the observed pitch variation in binary and ternary mixtures can be explained satisfactorily with the pitch–concentration relationship we have formulated. The obtained molecular twisting powers show wide variation for different liquid crystal molecules. Calculation of molecular twisting powers based on the actual dipolar and quadrupolar structure[3–5] of liquid crystal molecules would be very complicated; however, an attempt at a theoretical explanation of these as yet unpredictable molecular twisting powers should prove most interesting.

*This work was supported by the U.S. Army Research Office (Durham) under Grant No. DAHCO4-74-G-0186.

[1]C. S. Bak and M. M. Labes, J. Chem. Phys. 62, 3066 (1975).
[2]P. G. de Gennes, *The Physics of Liquid Crystals* (Clarendon, Oxford, 1974), Chaps. 3 and 6.
[3]W. J. A. Goossens, Mol. Cryst. Liq. Cryst. 12, 237 (1971).
[4]H. Stegemeyer, Ber. Bunsenges. Phys. Chem. 78, 860 (1974).
[5]H. Finkelmann and H. Stegemeyer, Ber. Bunsenges. Phys. Chem. 78, 869 (1974).
[6]J. Adams, G. Dir, and W. Haas, in *Liquid Crystals and Ordered Fluids*, edited by J. F. Johnson and R. S. Porter (Plenum, New York, 1974), Vol. 2, p. 421.
[7]In Ref. 5, measurements were carried out at 10 °C below the cholesteric–isotropic transition temperatures of the respective systems. However, in treating these data, we have made no correction for the temperature dependence of density (*d*), which one would expect to vary only slightly [see, for example, F. P. Price and J. H. Wendorff, J. Phys. Chem. 75, 2849 (1971)].

Effects of Molecular Complexing on the Properties of Binary Nematic Liquid Crystal Mixtures

Sir:

In order to achieve extended liquid crystalline temperature ranges, binary systems offer the advantage of frequently exhibiting eutectic behavior in their solid → mesophase transition while the mesophase → isotropic transition temperature varies linearly with composition. In particular, several binary nematic systems have been studied,[1-7] and only small deviations from linearity in the nematic → isotropic transition temperatures (T_{NI}) are noted when there are significant differences in molar volumes or densities of the components. This general behavior has been satisfactorily accounted for theoretically by Humphries and Luckhurst.[8]

It seemed to us that large deviations in T_{NI} as well as the solid → nematic transition temperature (T_{SN}) should be possible if molecular complex formation took place between the components of the binary system. Further, as opposed to the usual deviations in T_{NI} being depressions of the melting point,[9] in the case of complex formation, *increases* in the

Table I. Positive Deviations in T_{NI} for Binary Nematic Mixtures of CPB (Nematic Range 23.5–35.0°) and a Nematic Donor

Nematic donor	Nematic range of donor, °C	Mole % CPB	Nematic range of mixture, °C	ΔT_{NI}, °C
MBBA	20.9–43.5	46.0	37.5–49.2	+9.6
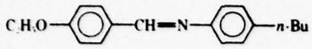	35.0–75.4	50.5	61.0–64.5	+9.5
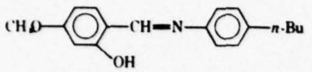	44.0–62.6	50.9	15.0–53.0	+4.5
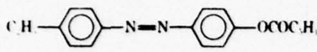	72.0–126.0	53.0	60.0–86.4	+8.6
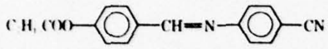	52.0–94.5	54.8	19.6–64.8	+2.9

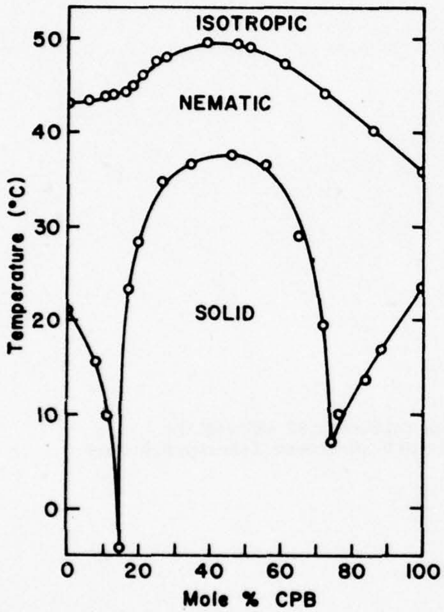

Figure 1. Phase diagram of MBBA–CPB.

melting point over either component of the system could occur. We have achieved this result in the binary system N-(p-methoxybenzylidene)-p-n-butylaniline (MBBA) and 4-cyano-4′-pentylbiphenyl (CPB) and several closely related binary mixtures.

MBBA and CPB were chosen[10] because of the possibility of a weak charge-transfer interaction between the components. Spectroscopic studies in the nematic phase of a 50–50 mole % binary mixture show a typical broad weak absorption band in the visible peaking at ~550 nm. The phase diagram (Figure 1) was determined using both polarized optical microscopy on a Mettler FP-2 hot stage and differential scanning calorimetry (DSC) utilizing a Perkin-Elmer DSC 1-B. DSC determinations were done on a heating cycle on samples which had been refrigerated at −20° for at least 5 days to avoid supercooled samples.

With regard to T_{SN}, the phase diagram is a classical example of a two-component system forming a compound, displaying a congruent melting point, and exhibiting two eutectics. T_{NI} shows a maximum at a temperature ~10° higher than expected for a linear relationship between the clearing points of the two components. The T_{NI} and T_{SN} maxima occur at ca. 50–50 mole % of MBBA–CPB. Enthalpies of the solid–nematic transition (ΔH_{SN}) for the binary mixture are plotted in Figure 2, showing minimal values of ΔH_{SN} at compositions close to the 50–50 mixture. Similar positive deviations in T_{NI} are seen in mixtures of

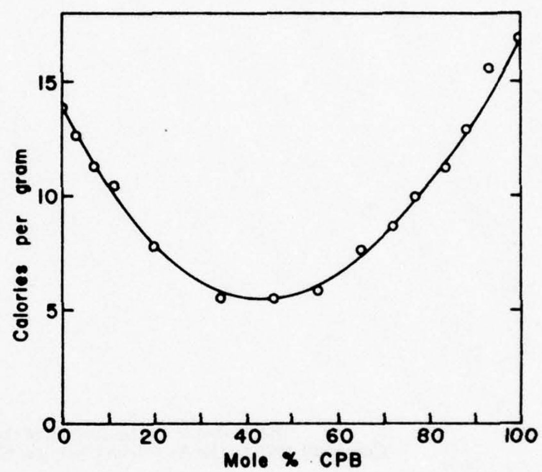

Figure 2. Heat of solid → nematic transition vs. mole % of CPB.

other Schiff bases or a nematic with a central azo linkage functioning as donor moieties with CPB functioning as the acceptor and are listed in Table I.

By virtue of charge-transfer interaction of components of a binary mixture, it is clear that extended liquid–crystalline temperature ranges can be achieved. The interaction also was expected to lead to nonlinearities in dielectric properties and possible modulation of electrooptical properties. Dielectric anisotropies were evaluated by measuring dielectric constants on aligned nematic samples, holding the orientation of the nematic director in a 15 kOe magnetic field.[11] Twisted nematic cells were constructed using SiO treated glass plates and 50 μ spacers to allow study of delay times, rise times, decay times, and threshold voltages (V_{th}) for electric field addressing in a manner previously described.[12]

Strong positive deviations in the value of $\Delta\epsilon$ ($=\epsilon_{\parallel} - \epsilon_{\perp}$) were observed. A 50–50 mole % MBBA–CPB mixture has a $\Delta\epsilon$ of 7.7 whereas a simple additivity law implies a value of 5.8. The delay time decreases by a factor of 2 in going from 100% CPB to the 50–50 mixture, but rise times, decay times, and V_{th} are relatively insensitive to composition.

It therefore appears quite likely that, in addition to extending nematic ranges by involving complexing between the components of a binary mixture, one can cause changes in dielectric anisotropies, viscosities, and elastic constants which will affect electrooptic behavior in these systems. Attempts to design appropriate systems to take maximum advantage of nonlinearities in their properties are in progress.

Acknowledgment. This work was supported by the U.S. Army Research Office (Durham) under Grant No. DAHC04-74-G-0186.

References and Notes

(1) J. S. Dave and M. J. S. Dewar, *J. Chem. Soc.*, 417 (1954); 4305 (1955).
(2) R. Steinstrasser and L. Pohl, *Z. Naturforsch., Teil B*, **26**, 87 (1971).
(3) L. Pohl and R. Steinstrasser, *Z. Naturforsch. Teil B*, **26**, 26 (1971).
(4) R. A. Bernheim and T. A. Shuhler, *J. Phys. Chem.*, **76**, 925 (1972).
(5) J. Homer and A. R. Dudley, *J. Chem. Soc., Chem. Commun.*, 926 (1972).
(6) H. Arnold and H. Sackmann, *Z. Phys. Chem. (Leipzig)*, **213**, 145 (1960).
(7) E. C. H. Hsu and J. F. Johnson, *Mol. Cryst. Liq. Cryst.*, **20**, 177 (1973); **27**, 95 (1974).
(8) R. L. Humphries and G. R. Luckhurst, *Chem. Phys. Lett.*, **23**, 567 (1973).
(9) The only exception is a binary mixture of *n*-butyl-*p*-(*p*-ethoxyphenoxycarbonyl)phenylcarbonate and (*p*-ethoxyphenylazo)phenylheptanoate reported in ref 3 and 4; nematic ranges for the pure components are inconsistent in these two reports, and a positive deviation in T_{NI} for a 60–40 mole % mixture of between 16 and 4° is implied. It is doubtful that these two compounds were sufficiently pure to make the result meaningful.
(10) MBBA and CPB are both available commercially in special highly purified grades suitable for electrooptic studies from Eastman Kodak Co. and Atomergic Chemetals Co., respectively.
(11) A. I. Baise and M. M. Labes, *Appl. Phys. Lett.*, **24**, 298 (1974).
(12) C. S. Bak, K. Ko, and M. M. Labes, *J. Appl. Phys.*, **46**, 1 (1975).

J. W. Park, C. S. Bak, M. M. Labes*
Department of Chemistry, Temple University
Philadelphia, Pennsylvania 19122
Received April 15, 1975

Mol. Cryst. Liq. Cryst., 1975, Vol. 31, pp. 355–357

Research Note

On the Helical Twisting Power of α-Phenethylamine in Nematic Liquid Crystals†

J. W. PARK and M. M. LABES
Department of Chemistry, Temple University, Philadelphia, Pennsylvania 19122

(*Received April 28, 1975; in final form May 19, 1975*)

It is the purpose of this Note to point out that the extraordinarily high helical twisting power reported for (+) and (−) forms of α-phenethylamine (PEA) dissolved in Schiff base-type nematic liquid crystals[1,2] is solely due to amine exchange reactions.

It is well known that chiral solutes, in general, induce cholesteric behavior in nematic liquid crystals,[3–5] and that if one substitutes a chiral center into a nematogen, a "chiral nematic" liquid crystal results with optical properties identical to conventional cholesteric liquid crystals.[6] Small optically active solute molecules produce minor perturbations of a nematic array, and the helical twisting power (defined as the reciprocal helix pitch extrapolated to 100% solute concentration[3]) is smaller than that of a typical cholesteric or chiral nematic molecule. The only exception is PEA[1,2] for which the helical twisting power has been reported to be higher than that of cholesteryl chloride.

PEA reacts rapidly at room temperature with N-(*p*-methoxybenzylidene)-*p*-*n*-butylaniline or its *p*-ethoxy-analog (EBBA).[7] The expected reaction product of EBBA and PEA was readily prepared by refluxing *p*-ethoxybenzaldehyde and (−) PEA in ethanol (Structure I below, EBPEA; infrared and nmr spectra consistent with structure). As can be seen from Figure 1, the high helical twisting power of PEA can easily be explained by amine exchange according to the reaction:

† This work was supported by the U.S. Army Research Office (Durham) under Grant No. DAHC04-74-G-0186.

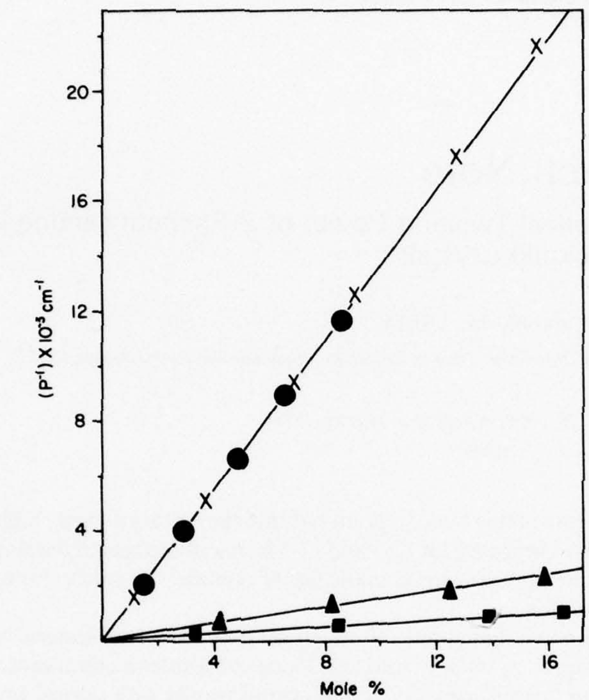

FIGURE 1 Reciprocal pitch vs mole % of solutes. PEA in Nematic Phase V (■); PEA in EBBA (●); EBPEA in EBBA (×); and α-phenethyl-alcohol in EBBA (▲). Nematic Phase V is a eutectic mixture of *p*-methoxyazoxybenzenes which are *p'* substituted with ethyl and *n*-butyl groups; it is commercially available from E. Merck.

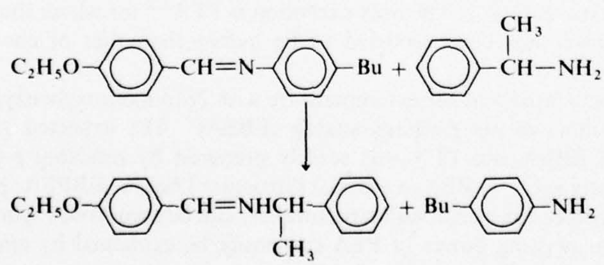

(I)

PEA in other nematic solvents that undergo no reaction has a normal helical twisting power and the structurally related α-phenethylalcohol has a comparable twisting power in EBBA, as can be seen in Figure 1.

NMR spectra of EBBA, EBPEA and a 1:1 mixture of PEA and EBBA were taken and the equilibrium constant for the amine exchange reaction, calculated from the ratio of aldehydic proton peaks in the mixture, is about 5.5 at room temperature. EBPEA is *not* a nematic liquid crystal (m.p. 33.6°) but its similarity in shape to nematogenic Schiff bases undoubtedly leads to substantial cooperativity in its interaction with them and the concomitant high helical twisting power.

References

1. H. Finkelmann and H. Stegemeyer, *Ber. Bunsenges. physik. Chem.*, **78**, 869 (1974).
2. E. H. Korte, S. Bualek, and B. Schrader, *Ber. Bunsenges. physik. Chem.*, **78**, 876 (1974).
3. H. Baessler and M. M. Labes, *J. Chem. Phys.*, **52**, 631 (1970).
4. A. D. Buckingham, G. P. Ceasar and M. B. Dunn, *Chem. Phys. Letters*, **3**, 540 (1969).
5. W. J. A. Goossens, *Mol. Cryst. Liq. Cryst.*, **12**, 237 (1970).
6. See, for example, D. Dolphin, Z. Muljiani, J. Cheng, and R. B. Meyer, *J. Chem. Phys.*, **58**, 413 (1973).
7. For studies of kinetics of closely related exchange reactions, see, B. A. Porai-Koshits and A. L. Remizov, *Probl. Mekhanizma Org. Reaktsii, Akad. Nauk Ukr. SSR, Otdel Fiz-Mat. i Khim. Nauk*, 238 (1953); *Chem. Abstr.*, **50**, 16686 (1956).

Self-diffusion coefficients of a nematic liquid crystal via an optical method

H. Hakemi and M. M. Labes

Department of Chemistry, Temple University, Philadelphia, Pennsylvania 19122
(Received 29 May 1975)

By observing the textural changes caused when an enantiomer is allowed to diffuse into a racemic nematic liquid crystal of the substituted phenyl-4-benzoyloxybenzoate series, self-diffusion coefficients can be directly evaluated in both the nematic and isotropic phases. The data obtained are shown to be consistent with other determinations by mass-transport techniques, but inconsistent with relaxation methods, and the mechanistic factors causing these inconsistencies are discussed.

INTRODUCTION

Recently we reported a new optical method for studying anisotropic diffusion in liquid crystals, and applied the technique to the determination of the diffusion coefficient of a cholesteryl ester into a nematic liquid crystal in both the nematic and isotropic phases.[1] Since diffusant and solvent were different size molecular species, it was necessary to estimate self-diffusion coefficients by making a correction for the mass discrepancies. A better case to examine would be that of a nematic compound having a single asymmetric carbon atom, so that a racemic form would behave like a nematic material, and either enantiomer would behave like a "chiral nematic" or cholesteric liquid crystal. In studying the diffusion of an enantiomer into a racemic form, the only difference between the molecules involved is in their optical properties; thermodynamically and structurally they are essentially equivalent, and thus one can approximate self-diffusion very accurately.

The existence of "chiral nematic" compounds has been recognized since the early days of liquid crystal research,[2] although the term chiral nematic was only recently introduced[3] to describe molecules which do not have the steroidal moiety and do have dielectric and viscoelastic properties more like a nematic, albeit their optical properties are identical to those of cholesterics. Examples of such chiral nematics have been prepared involving 4-(2-methylalkoxy) biphenyl derivatives,[4,5] Schiff bases having an optically active 2-methylbutyl group[2,3,6–9] or 1-deuteriobutoxy group[10] and 2-methylbutyl substituted phenylbenzoates and phenyl-4-benzoyloxybenzoates.[11–14] We selected for the diffusion study one of the compounds of the substituted phenyl-4-benzoyloxybenzoate series[14] which has a particularly wide liquid crystalline temperature range and is of high chemical stability. Its structure is given below.

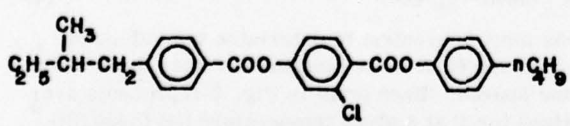

We will refer to the racemic form of this compound as ±PBOB. Of the several geometries and boundary conditions previously employed,[1] in this study ±PBOB was aligned uniaxially and homogeneously and a point source of +PBOB was allowed to diffuse radially. An ellipsoidal pattern develops from which both $D_\parallel$ and $D_\perp$ can be determined simultaneously.

EXPERIMENTAL

The preparation and properties of ±PBOB and +PBOB have been previously described.[14] ±PBOB had a nematic range of 45.0 – 91.9°; +PBOB had a cholesteric range of 40.0–86.4°. Whether these differences in ranges were due to purity differences or inherent in the properties of ± and +PBOB has not been determined.

The nematic material was placed between two silicon monoxide coated glass plates, $1\frac{1}{4}$ in. in diameter, separated by a 12.7 μm thick Mylar spacer, and cut so as to provide a 2 cm diameter circular path. The top plate had been drilled with a sand jet to produce a hole of ~150 μm diameter. The chiral nematic material was introduced into the hole after good uniaxial homogeneous alignment of ±PBOB was verified optically. Temperature control was achieved using a brass cell previously described;[1] the cell was placed in the gap of a 9 in. electromagnet and a field of 10 kOe was applied parallel to the glass plates (and also parallel to the long molecular axes of ±PBOB molecules).

At this field strength *no* cholesteric texture is formed since one is above the critical field for the cholesteric-nematic transition. When the field is removed, the cholesteric texture develops immediately, and an elliptical pattern of variably spaced Grandjean lines appear. The degree of ellipticity is a measure of the ratio $D_\parallel / D_\perp$, whereas the diffusion coefficient can be calculated from the distances between the variably spaced Grandjean lines. Measurements of the diffusion coefficients in the isotropic phase were conducted by quenching the sample to a temperature in the nematic phase, whereupon a circular pattern of variably spaced Grandjean lines was obtained. The diffusion gradients and Grandjean lines were measured at magnifications of 25× and 125× through a Nikon LKE microscope with crossed polarizers.

RESULTS

Figure 1 presents a photograph of the observed texture when +PBOB diffuses radially into ±PBOB showing diffusion ⊥ to the long molecular axis. The Grandjean lines are disclination lines between domains where the pitch jumps in a quantized way from k half-turns to $k+1$ half-turns. They are observed at equidistant intervals in a wedge type sample of a fixed concentration of cholesteric where the gap in the wedge traverses multiple integers of the half-pitch. The local half-pitch $P/2$ in each do-

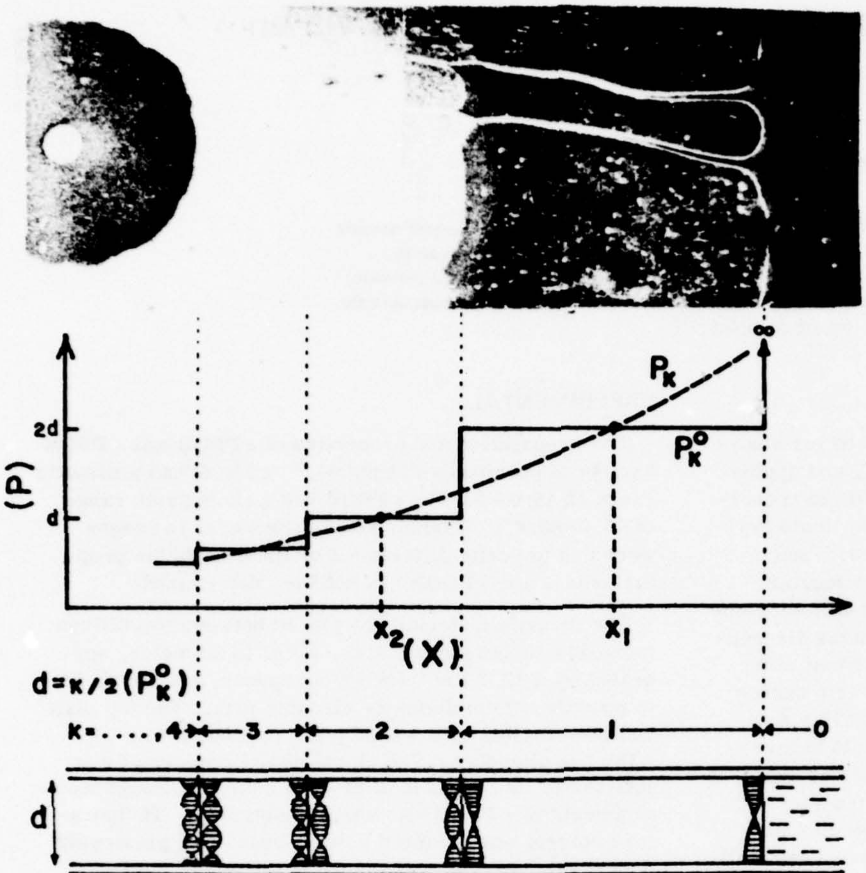

FIG. 1. Diffusion of - PBOB into uniaxially and homogeneously aligned ± PBOB. The point source (small white circle) at the left of the photograph has a diameter of 150 μm, and the short axis ($D_\perp$) of the elliptical diffusion pattern is shown. In the drawing, the quantized pitch jumps P_k^0 are represented by the solid line, whereas the pitch P_k is represented by the dashed line.

main is related to the local thickness d by $P/2 = d/k$, where k is an integer.[15] Similarly, in a fixed thickness sample with a concentration gradient, variably spaced Grandjean lines appear when the pitch jumps.[16] In each domain the local pitch P_k^0 is given by

$$d = \tfrac{1}{2} k P_k^0 , \tag{1}$$

where k is an integer ($k = 0, 1, 2, 3 \ldots$). In reality there are small perturbations of P_k going from Grandjean line to Grandjean line while the observed pitch P_k^0 is constant between these lines. The *midpoint* between lines is a better approximation for the distance x_k from the source at which the concentration C_k is defined by

$$C_k = \gamma / P_k , \tag{2}$$

where γ is an experimentally determined value for the linear relationship between C and $1/P$. This is pictorially represented in Fig. 1.

In our earlier work on a cholesteryl ester diffusing into N-(p-methoxybenzylidene)-p-n-butylaniline (MBBA), we incorrectly made the assumption that the half-pitch precisely at the Grandjean line was an integral multiple of the thickness; all the values of $D_\parallel$ in that work need to be corrected to be lower by a factor of ~1.5. The correction does not affect the values of the activation energies but does affect the values of the anisotropies $D_\parallel / D_\perp$. $D_\parallel / D_\perp$ was reported to be ~3 at 24.5°: its value should be ~2 at 24.5°. This makes less serious the discrepancy with the observed anisotropy in an elliptical diffusion pattern obtained for uniaxially and homogeneously aligned MBBA of 1.5 ± 0.2 and Rondelez' value[17] of 1.6.

For diffusion from a point source into an infinite plane surface, the solution of Fick's law is given by[18]

$$C = (M / 4\pi D t) \exp(-x^2 / 4Dt) , \tag{3}$$

where C is the concentration of the diffusant at a distance x from the source at time t, M is the total amount of material diffusing, and D is the concentration-independent diffusion coefficient. As shown in our previous work, substituting (1) and (2) into (3), the self-diffusion coefficient can be determined by measuring x_k at a time t from the equation

$$\ln k = \text{const} - x_k^2 / 4Dt . \tag{4}$$

It was most convenient to determine two values of x_k and k from the first three disclination lines developing from the source. Each point in Fig. 2 represents average values for D at a given temperature but three different anneal times t in the nematic phase. In the isotropic phase, no error bars are given since the experiments were done at only one anneal time. Table I gives the numerical values of the nematic phase diffusion coefficients, the diffusion anisotropy, and the calculated D_0 for the disoriented liquid. The experimental activation energies Ea for $D_\parallel$ and $D_\perp$, evaluated from the slope

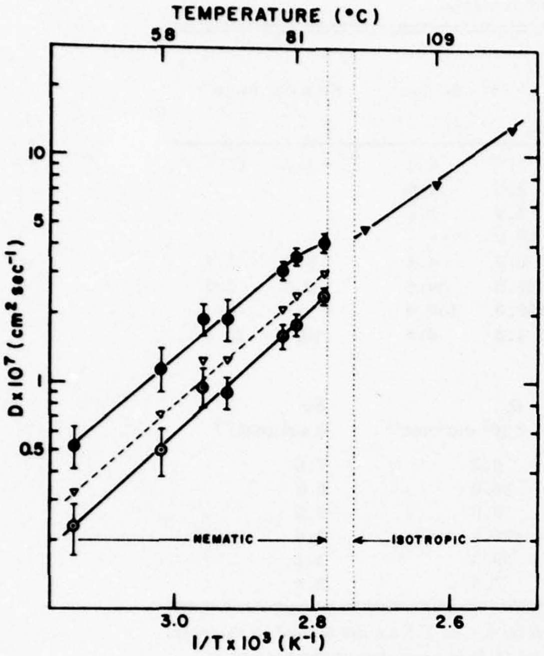

FIG. 2. Temperature dependence of the diffusion coefficients of PBOB in the nematic phase [●, $D_\parallel$; ○ $D_\perp$; ▽, $D_0 = 1/3(2D_\perp + D_\parallel)$] and in the isotropic phase.

of the curves in Fig. 2, are the same within experimental error (13.0 ± 1.0 kcal mole^{-1}) while D_0 in the isotropic phase is somewhat lower (9.3 ± 2.1 kcal mole^{-1}). Close to the nematic–isotropic transition temperature, $D_\parallel$ tends to be temperature independent, but measurements cannot be performed very close to this transition temperature with assurance of retaining a uniformly aligned nematic phase.

DISCUSSION

Self-diffusion coefficients can be measured by two fundamentally different techniques involving studies of mass transport or relaxation times. In molecular solids, excellent agreement exists among studies by the first technique, but relaxation studies are inconsistent among themselves and with the mass-transport studies, except in cases where a relatively simple vacancy diffusion process occurs.[19] In liquid crystals, the same situation prevails, particularly in light of the difficulties in the classical nuclear magnetic resonance (NMR) technique associated with very short relaxation times T_2. The values for the self-diffusion coefficient in MBBA and p-azoxyanisole (PAA) determined by these methods and neutron-scattering methods (NS) have been notoriously inconsistent and generally higher in magnitude than those determined by mass-transport methods.

In Table II, a comparison is given of typical data on three liquid crystal systems: MBBA[1,17,20–22] and its (partially) deuterated analog (DMBBA),[23] PAA,[24–26] and the compound studied in this work, PBOB. Focusing on mass-transport methods, there is a consistency in the data—all three systems have diffusion coefficients with anisotropies $D_\parallel/D_\perp$ of 1.5 to 2.3; D_0 undergoes no observable discontinuity at the transition from the nematic to isotropic phases. The mass-transport methods employed are of four different tracer types: the optical method (OT) described in this work; a diffusing-dye method (DT); C-14 labeled molecules (CT); and tritium diffusion (TT). Further, the values of D are roughly consistent with viscosity data, i.e., PAA which has a considerably lower viscosity than MBBA has a considerably higher D. No measurements of the viscosity of PBOB have been reported, but based on electro-optic studies, its viscosity is similar to and probably slightly greater than that of MBBA.[27]

In studies by the optical method of MBBA, we reported[1] that $D_\parallel$ was essentially temperature independent over the (short) nematic temperature range studied of 22 to 33°; from our data on PBOB, it appears most likely that $D_\parallel$ becomes relatively temperature independent close to the nematic–isotropic transition, but in a broader temperature range nematic material $D_\parallel$ ultimately shows the same activated temperature dependence as $D_\perp$. This latter result is consistent with Yun and Fredrickson's data on PAA.[24] In PBOB, D_0 shows a small change in activation energy going from nematic to isotropic phases, whereas in PAA and MBBA, Ea does not change.

The unreliability of relaxation methods in these systems is probably not entirely due to experimental difficulty. A multiple-pulse line narrowing technique which determines D from the dependence of the spin echo amplitude on the applied magnetic field gradient was developed recently to combat the experimental difficulties in measuring T_2.[21] For MBBA, $D_\parallel$ at 21° was reported to be $2 \pm 1 \times 10^{-6}$ cm^2 sec^{-1}, approximately seven times larger than the mass-transport values. The temperature dependence of the anisotropy of D was then studied by the same technique for DMBBA, where $D_\parallel$ at 21° was found to be $\sim 1 \times 10^{-6}$, and where D_0 was found to undergo a discontinuity at the phase transition, dropping by a factor of ~ 1.5.[23] These results are completely inconsistent with the mass-transport studies on three liquid crystals.

The inconsistencies probably arise as a consequence of a complex mechanism of diffusion. In normal liquids, thermal agitation causes molecules to translate and rotate in a random fashion, but some cooperativity can ex-

TABLE I. Self-diffusion coefficients $D_\parallel$, $D_\perp$, and D_0, and the anisotropy $D_\parallel/D_\perp$ in the nematic phase of PBOB.

	$D\times 10^7$ cm^2 sec^{-1}			
T(°C)	$D_\parallel$	$D_\perp$	$D_0 = 1/3(2D_\perp + D_\parallel)$	$D_\parallel/D_\perp$
45.0	0.52	0.23	0.32	2.25
58.0	1.15	0.50	0.71	2.30
64.5	1.90	0.95	1.25	2.00
69.0	1.90	0.90	1.25	2.10
78.5	3.10	1.60	2.10	1.94
81.0	3.60	1.80	2.40	2.00
86.0	4.10	2.40	3.00	1.70

TABLE II. Self-diffusion parameters for nematic liquid crystals.

Nematic phase							
				$D_{self} \times 10^7$ cm^2 sec^{-1}		Ea k cal mole^{-1}	
Compound	Method	Reference	Temp.	$D_\parallel$	$D_\perp$	$\parallel$	$\perp$
MBBA	OT	1	24.5	2.7[a]	1.3	~1.0	17.0
	DT	17	22.0	2.6	1.6		
	TT	20	25.0	>5.0	3.5		
	NMR	21	21.0	20.0	...		
DMBBA	NMR	23	5.0	6.9	4.6	5.0	5.4
PAA	CT[b]	24	125.0	45.3	29.6	3.5	2.6
	NS	25	125.0	180.0	100.0	...	...
PBOB	OT	this work	69.0	1.9	0.9	13.0	13.0

Isotropic phase					
Compound	Method	Reference	Temp. °C	D_0 $\times 10^7$ cm^2 sec^{-1}	Ea k cal mole^{-1}
MBBA	OT	1	44	6.0	8.0
	NMR	22	43	10.0	6.0
DMBBA	NMR	23	39	8.0	9.5
PAA	NS	26	136	170.0	3.0
	CT[b]	24	136	39.5	3.5
PBOB	OT	this work	109	7.5	9.3

[a]Data from Ref. 1 regarding $D_\parallel$ has been corrected by a factor of 1.5 as discussed in the text.
[b]Data from Ref. 24 has been corrected to give the values of D at an order parameter of 1. See C. K. Yun, Ph. D. thesis, University of Minnesota, 1970, p. 288.

ist as a short-range interaction. In liquid crystals, rotational motion is further suppressed while translational motion is still considerably more free than in a typical molecular solid. Even for liquids, it has been proposed that two modes of diffusion are involved. For example, Nir and Stein[28] have combined Eyring's theory of lattice diffusion with the Einstein–Sutherland equation for flow diffusion, and shown better agreement with experimental values in liquids than either theory alone.

In the liquid crystal phase, the importance of the order parameter, and the different nature of the boundary conditions used in diffusion experiments may be responsible for the discrepancies. Here again, mass-transport studies seem consistent, even though Yun and Fredrickson's experiments[24] involve larger samples and less-stringent alignment than utilized in the present studies. The curvature of the Arrhenius plots in the mass-transport studies is also indicative of the existence of more than one mechanism. It appears likely, then, that both latticelike and flowlike mechanisms are involved in mesophase diffusion and that mass-transport methods and relaxation methods are therefore monitoring different aspects of the diffusive motion. At present, mass-transport data are the only reliable and consistent information available on this interesting aspect of liquid-crystalline behavior.

ACKNOWLEDGMENTS

We wish to thank Dr. B. H. Klanderman of Eastman Kodak Company for information regarding PBOB. Helpful discussions with Drs. Z. Luz and S. Shtrikman of the Weizmann Institute are also gratefully acknowledged, as well as their assistance in providing precision-drilled glass plates. This work was supported by the U. S. Army Research Office (Durham) under Grant No. DAHCO4-74-G-0186.

[1]H. Hakemi and M. M. Labes, J. Chem. Phys. 61, 4020 (1974).
[2]G. Friedel, Ann. Phys. (Paris) 18, 273 (1922).
[3]D. Dolphin, Z. Muljiani, J. Cheng, and R. B. Meyer, J. Chem. Phys. 58, 413 (1973).
[4]M. Leclerq, J. Billard, and J. Jacques, C. R. Acad. Sci. Paris C 266, 654 (1968).
[5]G. W. Gray, K. J. Harrison, J. A. Nash, and E. P. Raynes, Electron. Lett. 9, 616 (1973).
[6]M. Leclercq, J. Billard, and J. Jacques, Mol. Cryst. Liq. Cryst. 8, 367 (1969).
[7]G. W. Gray, Mol. Cryst. Liq. Cryst. 7, 127 (1969).
[8]J. A. Castellano, R. N. Friel, M. T. McCaffrey, D. Meyerhofer, C. S. Oh, E. F. Pasierb, and A. Sussman, "Liquid Crystal Systems for Electro-optical Storage Effects," Air Force Materials Laboratory Report No. PRRL-71-CR-35, 1971.
[9]J. A. Castellano, E. F. Pasierb, C. S. Oh, and M. T. McCaffrey, "Electronically Tuned Optical Filters," Langley Research Center NASA Report No. NASA CR-112032, 1972.
[10]G. W. Gray, Mol. Cryst. Liq. Cryst. 21, 161 (1973).
[11]J. P. Van Meter and B. H. Klanderman, J. Am. Chem. Soc. 95, 626 (1973).
[12]J. P. Van Meter and B. H. Klanderman, Mol. Cryst. Liq. Cryst. 22, 271 (1973).
[13]J. P. Van Meter and B. H. Klanderman, Mol. Cryst. Liq. Cryst. 22, 285 (1973).
[14]B. H. Klanderman and T. R. Criswell, J. Am. Chem. Soc. 97, 1585 (1975).
[15]For a discussion of Grandjean lines in wedge type samples, see P. G. de Gennes, *The Physics of Liquid Crystals* (Clarendon, Oxford, 1974), p. 261.
[16]H. Kelker, Mol. Cryst. Liq. Cryst. 15, 347 (1972).
[17]F. Rondelez, Solid State Commun. 14, 815 (1974).
[18]J. Crank, *The Mathematics of Diffusion* (Oxford University,

London, 1956).
[19]See J. N. Sherwood in *Surface and Defect Properties of Solids*, (The Chemical Society, London, 1973), Vol. 2, p. 250.
[20]I. Teucher, H. Baessler, and M. M. Labes, Nat. Phys. Sci. 229, 25 (1971).
[21]R. Blinc, J. Pirs, and I. Zupancic, Phys. Rev. Lett. 30, 546 (1973).
[22]S. R. Ghosh and E. Tettamanti, Phys. Lett. A 34, 361 (1973).
[23]I. Zupancic, J. Pirs, M. Luzar, R. Blinc, and J. W. Doane, Solid State Commun. 15, 227 (1974). These authors worked with partially deuterated MBBA, and claim a nematic range for this compound of 3–33 °C, a surprisingly large change from the nematic range of MBBA itself.
[24]C. K. Yun and A. G. Fredrickson, Mol. Cryst. Liq. Cryst. 12, 73 (1970).
[25]J. A. Janik, J. M. Janik, K. Otnes, and T. Riste, Mol. Cryst. Liq. Cryst. 15, 189 (1971).
[26]K. Otnes, R. Pynn, J. A. Janik, and J. M. Janik, Phys. Lett. A 38, 335 (1972).
[27]B. H. Klanderman (private communication).
[28]S. Nir and W. D. Stein, J. Chem. Phys. 55, 1598 (1971).

Observation of Pyroelectricity in Chiral Smectic-*C* and -*H* Liquid Crystals*

L. J. Yu, H. Lee, C. S. Bak, and M. M. Labes
Department of Chemistry, Temple University, Philadelphia, Pennsylvania 19122
(Received 10 November 1975)

Pyroelectricity has been observed in the smectic-*C* and smectic-*H* phases of *l*-*p*-decyloxybenzylidene-*p*′-amino-2-methylbutylcinnamate after the material is poled in a dc field. The observed pyroelectric coefficient is consistent with an estimate of its theoretical value.

Recently Meyer *et al.*[1] have presented both theoretical arguments and some experimental evidence that *p*-decyloxybenzylidene-*p*′-amino-2-methylbutylcinnamate (DBC), when prepared as a pure enantiomer (using *l*-amyl alcohol), is ferroelectric in the smectic-*C* and smectic-*H* phases. It occurred to us that an indication of spontaneous polarization in these phases would be the presence of a *pyroelectric* effect. We have succeeded in measuring a pyroelectric current in the smectic-*C* and smectic-*H* phases of the *l*-enantiomer of DBC after aligning the phases in a dc electric field, and verified that no pyroelectric effect is observed in the racemic form of DBC.

l- and *dl*-DBC were synthesized in the following manner[2]: *p*-nitrocinnamic acid was converted to the acid chloride via treatment with thionyl chloride; *l*-amyl alcohol or *dl*-amyl alcohol was then added to form the *p*-nitrocinnamate ester,

which was reduced to the p-aminocinnamate ester with stannous chloride and hydrochloric acid. Finally, the Schiff base DBC was made by condensing the p-aminocinnamate ester with n-decyloxybenzaldehyde. The phase transition temperatures were in good agreement with those previously reported.[1]

The pyroelectric measurements were performed on samples of l-DBC and dl-DBC aligned between two glass plates which had been coated with indium oxide and then with silicon monoxide to promote homogeneous alignment.[3] A 6.3-μm or 12.7-μm Mylar film with a 1.2×1.2-cm^2 hole was used as a spacer. The samples were heated to 125°C, 8° higher than the isotropic transition temperature, kept under a dc electric field of 5×10^4 V cm^{-1} for 1 h, and quenched to the smectic-C phase with the field still applied. This treatment serves two functions: Undesirable ionic species are removed by electrolysis, and the sample is "poled"; i.e., the dipoles are aligned in the field. Alternatively, the sample can be poled starting from the smectic-A phase (115–95°C). In the smectic-C and -H phases, the "spontaneous" currents are measured after the "background" current stabilizes, which takes ~2 h. A small residual background current is always observed; in l-DBC a pyroelectric current is also observed when the sample is heated (or cooled) at a rapid heating (or cooling) rate. The pyroelectric currents were measured in the smectic-C and -H (<63°C) phases. In the smectic-A phase, in accord with theory, no pyroelectric current could be observed. However, the background current in this phase was always quite high, and it would therefore be difficult to distinguish a pyroelectric current in this phase in any event.

In the experiments reported in this work, the molecular axis is parallel to the glass; i.e., the smectic planes are perpendicular to the glass and an electric field is applied perpendicular to the glass plates. A macroscopic dipole moment will only occur when the helicoidal smectic array is "untwisted," i.e., when the pitch approaches infinity. We found that after poling, the infinite-pitch smectic-C and -H phases were partially retained for several hours even after the field was removed; i.e., a memory state was achieved. Microscopic observations indicated that a large portion of the sample did not relax back to the so-called fingerprint texture; the helical array may be partially restored but with a large pitch.[4] For this reason, the structures of both the smectic-C and the smectic-H phases, being untwisted, should have a macroscopic dipole moment and should therefore show a pyroelectric effect. As a control experiment dl-DBC was treated in an identical manner; because of the apolar character of this material, no pyroelectric effect should be observable.

Pyroelectric currents were measured in a manner previously described.[5] The samples are first held at a fixed temperature until a stable background current is observed and recorded; heating rates of 75 and 10°/min for the smectic-C and smectic-H phases, respectively, were applied and the phases heated to a 5° higher temperature. As can be seen in Fig. 1, this heating produces a current pulse as well as a rise in the background current. The background current stabilizes again as soon as the temperature stabilizes. When no pyroelectric current is produced, as in the experiments with dl-DBC, one observes the rise in the background current, but no pyroelectric current pulse.

The pyroelectric coefficient dP/dT can be calculated from the data of Fig. 1 from the following expression for the pyroelectric current I:

$$I = A(dP/dT)dT/dt\,, \qquad (1)$$

where A is the electrode area and dT/dt is the heating rate. The highest value of the pyroelectric coefficient in the smectic-C phase is $\sim 2\times 10^{-11}$ C deg^{-1} cm^{-2}, and $\sim 3\times 10^{-11}$ C deg^{-1} cm^{-2} in the smectic-H phase. The magnitude of the ob-

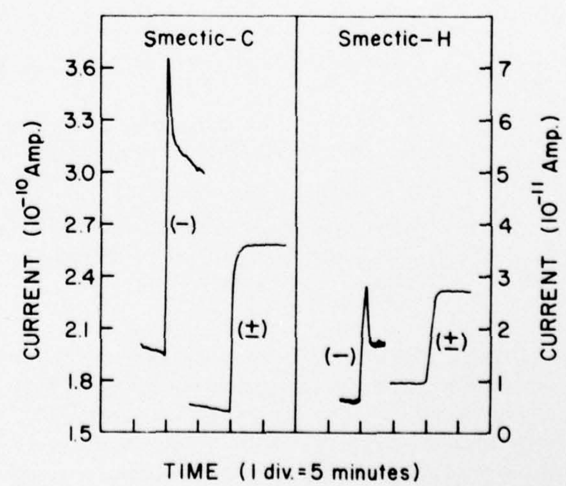

FIG. 1. Recorder tracings of observed currents in chiral (−) and racemic (±) DBC. The compounds are heated from 65 to 70°C at a rate of 75°/min in the smectic-C phase, and from 50 to 55°C at a rate of 10°/min in the smectic-H phase.

served pyroelectric coefficient was often as much as a factor of 2 less than this, the irreproducibility presumably related to the degree of alignment and memory state which exists in the individual sample.

An estimate of the theoretical value of dP/dT can be made in the following manner. Polarization P is defined as the macroscopic dipole moment per unit volume V:

$$P = N\bar{u}/V = \rho\bar{u}, \tag{2}$$

where N is the number of dipoles in the volume V, $\bar{u}$ is the dipole moment, and $\rho = N/V$. By differentiating Eq. (2) with respect to temperature T, one obtains

$$\frac{dP}{dT} = P\left(\frac{1}{\rho}\frac{d\rho}{dT} + \frac{1}{\bar{u}}\frac{d\bar{u}}{dT}\right). \tag{3}$$

The relative change in density $(1/\rho)d\rho/dT$ is approximately the volume expansion coefficient (negative sign) and should have the value of $\sim -1 \times 10^{-3}$ deg^{-1}.[6,7] The magnitude of the second term in Eq. (3) is -10^{-5} deg^{-1},[8] and can therefore be neglected.[9] P can be assumed[1] to have a value of ~ 125 esu cm^{-2} $(= 4.2\times 10^{-8}$ C cm$^{-2})$. Therefore an estimate of dP/dT is $\sim -4\times 10^{-11}$ C deg^{-1} cm^{-2}.

Thus the observed value of the pyroelectric coefficient $[(2 \text{ to } 3)\times 10^{-11}$ C deg^{-1} cm$^{-2}]$ is quite close to the theoretical value. Since neither perfect alignment of smectic-C and -H phases nor perfect untwisting of the chiral phases can be assured, the agreement is rather good. Further work on describing the properties of these interesting phases is underway.

---

*This work was supported by the U. S. Army Research Office under Grants No. DAHC04-74-G-0186 and No. DAAG29-76-G-0040.

[1]R. B. Meyer, L. Liebert, L. Strzelecki, and P. Keller, J. Phys. (Paris), Lett. 36, L-69 (1975).

[2]M. Leclercq, J. Billard, and J. Jacques, Mol. Cryst. Liq. Cryst. 8, 367 (1969); A. Psarrea, C. Sandris, and G. Tsatsas, Bull. Soc. Chim. Fr. 1961, 2145.

[3]J. L. Janning, Appl. Phys. Lett. 21, 173 (1972).

[4]The lifetime of such a memory state seems to depend on the thickness and boundary conditions of the sample. Although Meyer *et al.* (Ref. 1) did not report memory effects in their earlier work, observations of long-lived untwisted states have also been made by them (R. B. Meyer, private communication).

[5]A. I. Baise, H. Lee, B. Oh, R. E. Salomon, and M. M. Labes, Appl. Phys. Lett. 26, 428 (1975).

[6]L. E. Hajdo, A. C. Eringen, A. E. Lord, Jr., and F. E. Wargocki, Lett. Appl. Eng. Sci. 3, 125 (1975).

[7]L. E. Hajdo, A. C. Eringen, J. Giancola, and A. E. Lord, Jr., Lett. Appl. Eng. Sci. 3, 61 (1975).

[8]R. G. Kepler, in "Proceedings of the Second International Conference on Electrophotography, October 1973" (Society of Photographic Scientists and Engineers, to be published).

[9]The polarization is expected to change rapidly near the smectic-C–smectic-A transition temperature [see, for example, R. Blinc, Phys. Status Solidi (b) 70, K29 (1975)]. Our measurements for the smectic-C phase were therefore carried out 20° below this transition point to avoid any contribution to the current from such a pretransitional phenomenon.

ELECTRIC FIELD INDUCED TRANSFORMATIONS AND STRUCTURAL EXPLANATIONS OF LARGE PITCH CHOLESTERIC FINGERPRINT AND SPHERULITIC TEXTURES. A. E. Stieb* and M. M. Labes, Department of Chemistry, Temple University, Philadelphia, Pa., 19122, U.S.A.

Although there have been many studies of both fingerprint textures and bubbles (spherulitic textures) in cholesterics of large pitch, no complete explanation of their structures has been given. By studying the electric field induced transformation of bubbles and fingerprints and combining these data with wedge and diffusion-gradient observations, structural models consistent with several types of bubble and fingerprint patterns have been developed.

In the absence of an applied field, two different fingerprint patterns are observed, one of which has homeotropic regions separating the individual stripes, while the other pattern shows only bright focal lines. In the presence of a field, both patterns undergo continuous transformations to more complex structures involving disclinations. The dependence of the diameter of the fingerprint stripes and bubbles on the field strength is given for a cholesteric with positive dielectric anisotropy.

Bubbles of two types can be observed: one of them contains in its center a vertical disclination and is more stable than the other type, which has not been previously reported. The behavior of both types of bubbles in an electric field will be discussed, as well as a bubble to fingerprint transformation.

The optical properties of all of these patterns were investigated in detail; structural models consistent with the experimental observations will be presented.

*Visiting Research Associate, 1975-1976. Permanent address: Institut f. Angewandte Festkörper-Physik, Freiburg, W. Germany.

Dielectric, elastic, and electro-optic properties of a liquid crystalline molecular complex*

J. W. Park and M. M. Labes

Department of Chemistry, Temple University, Philadelphia, Pennsylvania 19122
(Received 11 August 1976)

The dielectric and elastic constants as well as the electro-optic response times of twisted nematic cells of the binary liquid crystalline system *N*-(*p*-methoxybenzylidene)-*p*-*n*-butylaniline (MBBA)/4-cyano-4′-pentylbiphenyl (CPB) were studied. The formation of a molecular complex between MBBA and CPB leads to wide mesomorphic ranges and higher dielectric anisotropies, as well as favorable rise and decay times. This latter effect is mainly due to relative decreases in viscosity at a given temperature associated with elevation of the nematic-isotropic transition temperature.

PACS numbers: 61.30.−v, 78.20.Jq, 77.20.+y

INTRODUCTION

In a previous paper,[1] the formation of molecular complexes in liquid crystalline systems such as *N*-(*p*-methoxybenzylidene)-*p*-*n*-butylaniline (MBBA) and 4-cyano-4′-pentylbiphenyl (CPB) and several closely related binary mixtures was reported. The phase diagrams showed depressions of solid-nematic transitions (a double eutectic) as well as increases in the nematic-isotropic transition temperature. Preliminary data indicated positive deviations in the value of the dielectric anisotropies $\Delta\epsilon$ $(=\epsilon_{\parallel}-\epsilon_{\perp})$ and decreases in the delay time for deformation of a twisted nematic cell. As these properties are quite different from those of ordinary liquid crystalline mixtures, which show linear variation in the dielectric anisotropies and constant elastic constants,[2-4] we decided to study in detail the properties of the MBBA-CPB system.

In order to assure strong coupling between an applied field and molecular orientation in a liquid crystal, a high dielectric anisotropy $\Delta\epsilon$ is desirable. Further, the time constants for reorientation (rise time) and relaxation (decay time) of the nematic director are both dependent on viscosity. Gruler *et al.*[5] calculated the relationship between geometry and threshold field for field-induced deformations of a nematic layer. In the case of a planar alignment and a positive dielectric anisotropy $(\Delta\epsilon>0)$, the threshold voltage (V_{th}) is

$$V_{th}=\pi(k_{11}/\epsilon_0\Delta\epsilon)^{1/2}, \tag{1}$$

where $K=k_{11}+\frac{1}{4}(k_{33}-2k_{22})$, and k_{ii} are the Frank elastic constants.[6] Above V_c, the orientation of the nematic director changes with the characteristic rise time τ_r and relaxes in a decay time τ_d given by the following expressions[9]:

$$V_c=\pi(K/\epsilon_0\Delta\epsilon)^{1/2} \tag{2}$$

where $K=k_{11}+\frac{1}{4}(k_{33}-2k_{22})$, and k_{ii} are the Frank elastic constants.[6] Above V_c, the orientation of the nematic director changes with the characteristic rise time τ_r and relaxes in a decay time τ_d given by the following expressions[9]:

$$\frac{1}{\tau_r}=\frac{\epsilon_0\Delta\epsilon E^2}{\eta}-\frac{K}{\eta}q^2, \tag{3}$$

$$\tau_d=\frac{\eta}{Kq^2}, \tag{4}$$

where E is the applied field strength, η is the viscosity, and q is not clearly known but is often approximated by π/L where L is the layer thickness.[10-12] In this work we report on the above-mentioned parameters as they vary over the phase diagram of MBBA-CPB.[1]

EXPERIMENTAL

MBBA and CPB were purchased from Eastman Kodak Co. and Atomergic Chemetals Co., respectively, in pure grades used for electro-optic applications, and mixtures were made by weighing the individual components. The electrical and electro-optical properties were measured in planar or twisted cells consisting of two glass plates coated with tin oxide separated by Mylar spacers. The spacing was either 36.1 or 8.8 μm. The cells were put into a brass jacket through which water could be circulated at constant temperature. Capacitance measurements were performed using a General Radio 1608-A impedance bridge. Control of the nematic director was achieved by applying a magnetic field of ~27 kOe. Cell spacings were calibrated for every cell by measuring the capacitance of air. Threshold voltages were calculated from capacitance-voltage measurements. The glass plates used in threshold-voltage and electro-optical property measurements were coated with silicon monoxide (SiO) to promote homogeneous and uniaxial alignment. Only freshly prepared SiO-coated cells were used. The cells were filled by capillary action and uniform alignment confirmed by microscopic examination and capacitance measurements. All cells used in the threshold voltage and electro-optical properties showed capacitance values which agree within 0.5% of those determined by aligning in the magnetic field. The response times of twisted nematic cells were measured in essentially the same way as described in Ref. 11. Most measurements were done at 10 °C below the nematic → isotropic transition temperature T_{NI} to minimize the effects of changes in the order parameter.

RESULTS

The values of the dielectric constant $\epsilon_{\perp}$ and the dielectric anisotropy $\Delta\epsilon$ of the various mixtures are plotted against mol% CPB in Fig. 1. The solid lines are calculated values assuming the additivity relationship

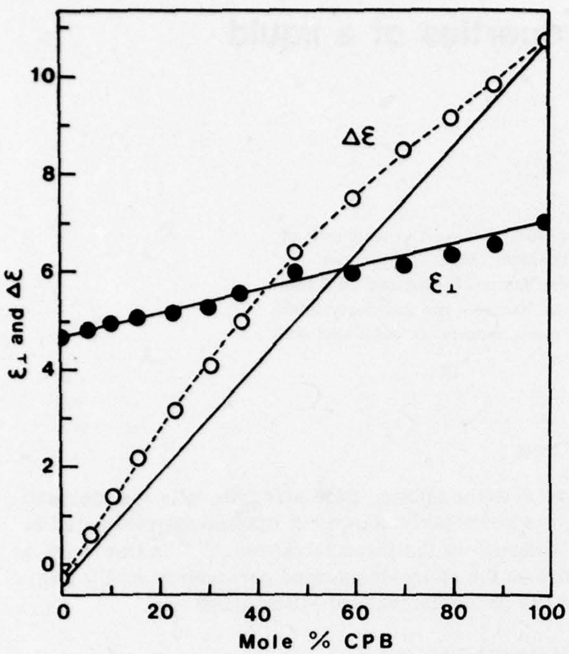

FIG. 1. $\epsilon_\perp^{mix}$ and $\Delta\epsilon^{mix}$ versus mol% CPB at 10 °C below the nematic-isotropic transition temperature. The solid lines are calculated from simple additivity relationships.

$$\epsilon_\perp^{mix} = \epsilon_\perp^{MBBA}(1 - X) + \epsilon_\perp^{CPB} X,$$

$$\Delta\epsilon^{mix} = \Delta\epsilon^{MBBA}(1 - X) + \Delta\epsilon^{CPB} X,$$

where X is the mole fraction of CPB. The actual values of $\epsilon_\perp$ show little deviation from this additivity relationship. On the other hand, $\Delta\epsilon$ shows large positive deviations with composition, which are obviously mainly due to the nonlinearity of $\epsilon_\parallel$.

Figure 2 is a plot of the elastic constant k_{11} which is calculated from Eq. (1) using V_{th} and $\Delta\epsilon$ values obtained from the capacitance-voltage relationships against mol% CPB. The $V_{th}^2\Delta\epsilon$ values are also given. The results indicate only a slight increase in k_{11} associated with complex formation. The k_{11} values of MBBA and CPB agree fairly well with those reported by other

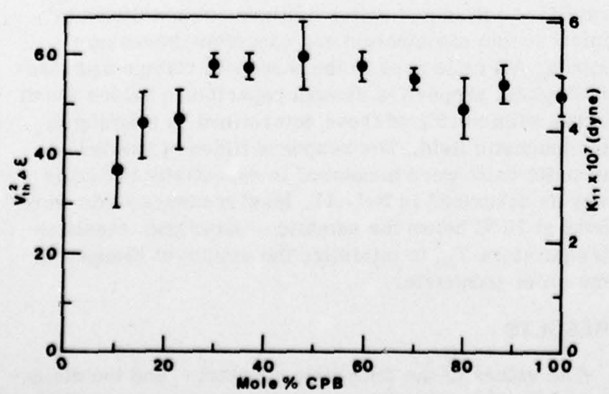

FIG. 2. $V_{th}^2\Delta\epsilon$ and k_{11} versus mol% CPB at 10 °C below the nematic-isotropic transition temperature.

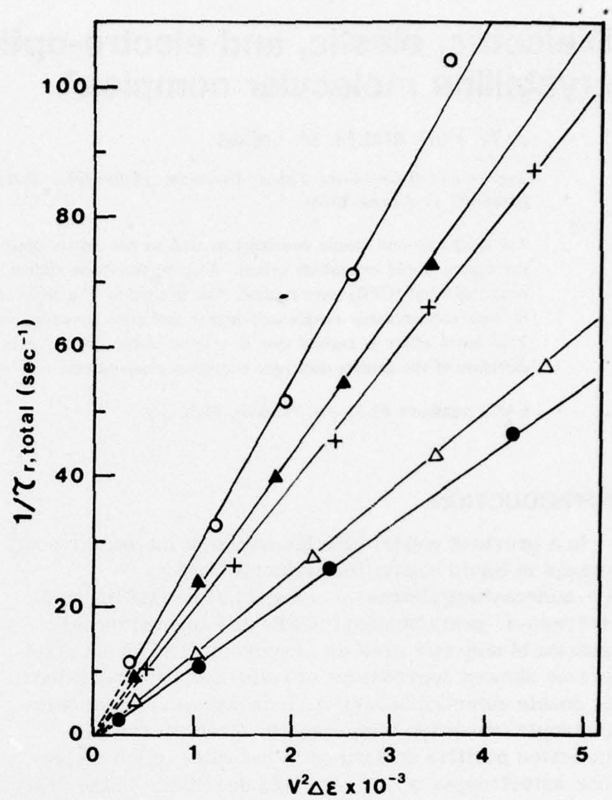

FIG. 3. Reciprocal total rise times versus $V^2\Delta\epsilon$ for various 36.1-μm-thick twisted nematic cells of CPB-MBBA mixtures. Proceeding from top to bottom, the curves were measured for the following mixtures and temperatures: 23.3 mol% CPB, 37.5 °C; 47.9 mol% CPB, 40 °C; 70.3 mol% CPB, 35 °C; 70.3 mol% CPB, 25 °C; pure CPB, 26 °C.

groups.[13,14] correcting for the temperature dependence of the elastic constant.

In Fig. 3, the reciprocal of the total rise time ($\tau_{r,total}$) is plotted against $V^2\Delta\epsilon$. The total rise time used in Fig. 3 and Table I is the time required to obtain

TABLE I. Electro-optic parameters of 36.1-μm-thick twisted nematic cells of MBBA-CPB.

	Mol% CPB				
Parameter	23.3	47.9	70.3	70.3	100.0
T (°C)[a]	37.5	40.0	35.0	25.0	26.0
$\Delta\epsilon$	3.14	6.36	8.48	8.70	10.7
V_c (V)	1.26	0.94	0.77	0.88	0.72
$V_c^2\Delta\epsilon$	5.0	5.7	5.0	6.7	5.5
$\tau_{r,total}$ (msec)[b]	30.8	17.5	15.1	23.0	21.3
τ_d (sec)[b]	0.53	0.61	0.66	0.84	1.04
$\frac{\Delta V^2\Delta\epsilon}{\Delta(\tau_{r,total}^{-1})}$ (V²sec)	39	44	51	77	88

[a] All data were taken at 10 °C below T_{NI}, with the exception of the data at 70.3 mol% and 25 °C, which is 20 °C below T_{NI}

[b] $\tau_{r,total}$ and τ_d were measured during and after application of 20 V.

Erratum: Dielectric, elastic, and electro-optic properties of a liquid crystalline molecular complex [J. Appl. Phys. 48, 22 (1977)]

J. W. Park and M. M. Labes

Department of Chemistry, Temple University, Philadelphia, Pennsylvania 19122

PACS numbers: 99.10.+g, 61.30.−v, 78.20.Jq, 77.20.+y

Following Eq. (1) on p. 22, the paragraph should read as follows: where k_{11} is the splay elastic constant.[6] The appropriate relationships for changing a twisted nematic texture to a homeotropic alignment are given by the following expressions in mks units.[7,8] The threshold voltage V_c is

[6] F.C. Frank, Discuss. Faraday Soc. 25, 19 (1958).
[7] F.M. Leslie, Mol. Cryst. Liq. Cryst. 12, 57 (1970).
[8] C.J. Alder and E.P. Raynes, J. Phys. D 6, L33 (1973).

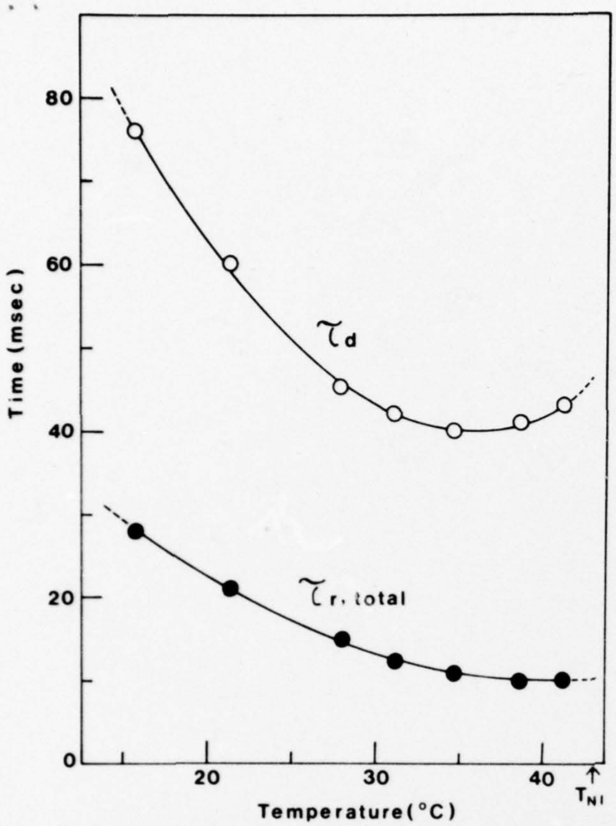

FIG. 4. Total rise and decay times of an 8.8-μm twisted nematic cell consisting of 71.3 mol% CPB and 29.7 mol% MBBA, at various temperatures. The applied voltage is 5.0 V.

90% light transmission after field is applied, and is the sum of the delay time and rise time.[11] Delay times were three to six times longer than rise times depending on composition and temperature. The linear dependence of $1/\tau_{r,\,total}$ on $V^2\Delta\epsilon$ is consistent with the theoretical prediction from Eq. (4) and other experimental results.[10-12] Decay time is defined as the time required to return to 10% light transmission after the voltage is turned off.

Various electro-optical properties and parameters are summarized in Table I. The parameter $\Delta(V^2\Delta\epsilon)/\Delta(\tau^{-1}_{r,\,total})$ is the inverse slope of the curves in Fig. 3 and is directly proportional to η, whereas τ_d is proportional to η/K.

Figure 4 shows the temperature variation of rise and decay times of an 8.8-μm twisted nematic cell consisting of 71.3 mol% CPB. The response times agree very well with the theoretical predictions given by Eqs. (3) and (4). In the whole nematic range (15–43 °C), the response times are much less than the 100 msec desirable for actual display applications. The shape of the curves can be understood in terms of the temperature dependences of the elastic constants, viscosities, and dielectric anisotropies.

CONCLUSIONS

The formation of a molecular complex between MBBA and CPB affords wide mesomorphic ranges as well as desirable modifications of the properties of the liquid crystalline phase such as $\Delta\epsilon$, η, and K. Useful display devices could be built with such a system since the electro-optic response times of a thin cell are <100 msec over the entire nematic range. The MBBA-CPB system represents no attempt at optimizing the changes in viscosity and dielectric anisotropies possible by virtue of a donor-acceptor interaction, nor does it indicate that elastic constants are responsive to such an interaction. Further work is underway designing mesogens which would show even more marked donor or acceptor properties.

*Work supported in part by the U.S. Army Research Office (Durham) under Grant No. DAHC04-74-G-0186.

[1]J.W. Park, C.S. Bak, and M.M. Labes, J. Am. Chem. Soc. **97**, 4398 (1975).
[2]R.A. Kashnow and H.S. Cole, Mol. Cryst. Liq. Cryst. **23**, 329 (1973).
[3]R.E. Michel and G.W. Smith, J. Appl. Phys. **45**, 3234 (1974).
[4]D. Meyerhofer, J. Appl. Phys. **46**, 5084 (1975).
[5]H. Gruler, T.J. Scheffer, and G. Meier, Z. Naturforsch. A **27**, 966 (1972).
[6]F.C. Frank, Discuss. Faraday Soc. **25**, 19 (1958).
[7]F.M. Leslie, Mol. Cryst. Liq. Cryst. **12**, 57 (1970).
[8]C.J. Alder and E.P. Raynes, J. Phys. D **6**, L33 (1973).
[9]E. Jakeman and E.P. Raynes, Phys. Lett. A **39**, 69 (1972).
[10]A.I. Baise and M.M. Labes, Appl. Phys. Lett. **24**, 298 (1973).
[11]C.S. Bak, K. Ko, and M.M. Labes, J. Appl. Phys. **46**, 1 (1975).
[12]T.S. Chang, P.E. Greene, and E.E. Loebner, *Liquid Crystals and Ordered Fluids*, edited by J.F. Johnson and R.S. Porter (Plenum, New York, 1974), Vol. 2, p. 115.
[13]I. Haller, J. Chem. Phys. **57**, 1400 (1972).
[14]P.G. Cummins, D.A. Dunmur, and R.A. Laidler, Mol. Cryst. Liq. Cryst. **30**, 109 (1975).

Mol Cryst Liq Cryst., Vol. 34 (Letters), pp. 147-152

Printed in the United States of America

BROADENING OF THE NEMATIC TEMPERATURE RANGE BY A NON-MESOGENIC SOLUTE IN A NEMATIC LIQUID CRYSTAL

J. W. PARK AND M. M. LABES
Department of Chemistry, Temple University, Philadelphia, Pennsylvania 19122

(Submitted for publication January 7, 1977)

Abstract The general rule that addition of a non-mesogenic solute causes a sharp decrease in the nematic-isotropic transition temperature ($T_{N\to I}$) of a nematic solvent is not obeyed when the solute and solvent can enter into a donor-acceptor interaction. Addition of 4-aminobiphenyl to the nematic liquid crystal 4-cyano-4'-pentylbiphenyl (nematic range ~ 25-35°) leads to an increase in $T_{N\to I}$ and a decrease in the crystal-nematic transition temperature. The maximum nematic range (21-38°) is achieved at ~ 7 mole % solute.

In order to extend liquid crystalline temperature ranges, it is common to prepare a mixed system to take advantage of eutectic behavior. In a typical binary mixture, where the components are miscible in all proportions, the phase diagram shows a nearly linear dependence of the nematic→isotropic (N→I) transition, and a simple eutectic determined by heats of melting of the components in the crystal→nematic (C→N) transition.

In a previous paper,[1] we reported unusual phase diagrams of binary liquid crystalline mixtures between 4-cyano-4'-pentylbiphenyl (CPB) and Schiff base or azo type liquid crystals: for example, when N-(p-methoxybenzylidene)-p-n-butylaniline (MBBA) is mixed with CPB, a double eutectic is found in the C→N transition and the N→I transition temperature increases as one proceeds from either component to an ~ equimolar mixture.

These unusual phase diagrams were attributed to a donor-acceptor type interaction between the constituent molecules. Further studies[2] of the MBBA-CPB system showed strong positive deviations in the dielectric anisotropies ($\Delta\varepsilon$) from a normal linear relationship, slight increases in the splay elastic constants, and marked decreases in the

electro-optic response times of twisted nematic cells made from the mixtures.

It occurred to us that similar type phase diagrams and changes in properties could be achieved when a non-mesogenic solute is dissolved in a liquid crystalline solvent *if* the solute and solvent undergo a donor-acceptor interaction. In general, addition of a non-mesogenic solute leads to a sharp decrease in $T_{N\to I}$ of a mesogenic solvent.[3-7] Such a decrease can be understood in terms of the degree of disruption of nematic order caused by the solute, which are functions of the size, shape and flexibility of the solute, and to any changes in dipole-dipole interactions or dispersion forces in the solvent caused by the solute. The slope of the depression of $T_{N\to I}$ ($\partial T_{N\to I}/\partial_X$, where X is the mole fraction of solute) is a measure of this perturbation.

Contrary to this general rule, we find that when 4-aminobiphenyl (ABP),[8] a non-mesogenic donor type molecule, is added to CPB, $T_{N\to I}$ increases and $T_{C\to N}$ decreases with a maximum nematic range being achieved at $\sim$ 7 mole % ABP. As opposed to pure CPB, which has a nematic range of 25-35°, 93% CPB/7% ABP has a range of 21-38°. The phase diagram (Figure 1), determined by using polarized optical microscopy on a Mettler FP-2 hot stage, and differential scanning calorimetry (DSC), utilizing a Perkin-Elmer DSC 1-B, is another example of a two-component system forming a compound showing a congruent melting point at a 50:50 mixture, and exhibiting two eutectics in the melting point. Enthalpies (ΔH) of the C→N or C→I transitions for the binary mixture are plotted in Figure 2, showing virtually linear variations of the total enthalpies of melting with composition. The complexity of Figures 1 and 2 can be explained in terms of definite compositions in the stable solid phases.

When 4-cyanobiphenyl (CBP), which is structurally similar to ABP, but bears a cyano group instead of an amino group, is mixed with CPB, a normal phase diagram of a two-component system with $(\partial T_{N\to I}/\partial_X)_{X=0}$ = -50° is obtained. Both ABP and CBP dissolved in nematic phase V (a eutectic mixture of p-methoxyazoxybenzenes which are p'-substituted with ethyl and n-butyl groups) induce sharp decreases in $T_{N\to I}$, giving $(\partial T_{N\to I}/\partial_X)_{X=0}$ values of -203 and -160° respectively. For a binary mixture between MBBA and CBP, $T_{N\to I}$ decreased approximately linearly with mole fraction of CBP with $(\partial T_{N\to I}/\partial_X)_{X=0}$ = -123°. However, the melting point curve showed a slight negative deviation from a smooth line near the 50:50 mixture.[9]

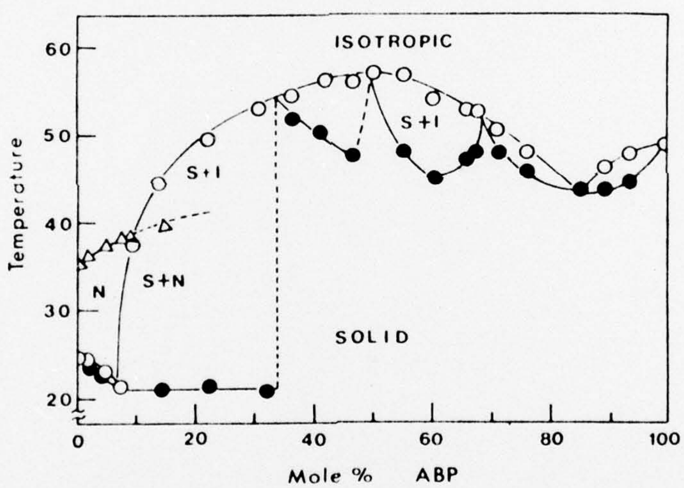

Figure 1. Phase diagram of CPB-ABP mixture: $T_{N \to I}(\Delta)$, melting point of last trace of solid (O), and melting point of excess components (●).

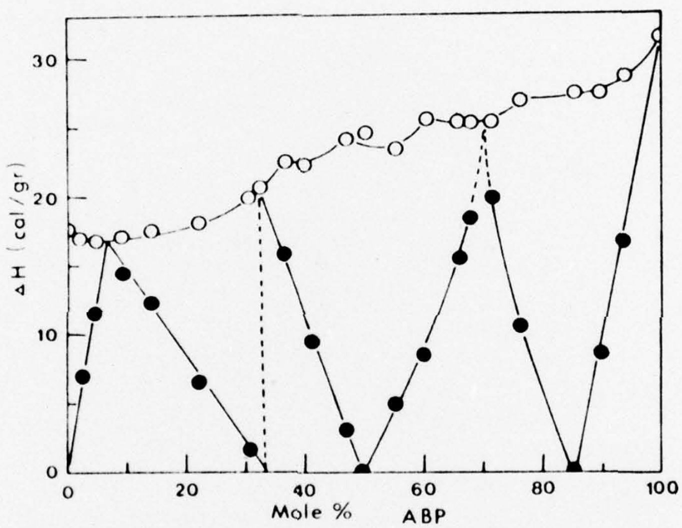

Figure 2. Heat of solid→nematic or liquid transition of CPB-ABP mixture: total heat of melting (○) and heat of melting of excess components (●).

These results clearly indicate that CPB and ABP form a complex. The complex may either be linear through the interaction between CN and NH_2 groups, or plate-like through the interaction between biphenyl rings. Either of these effects can lead to a $T_{N\to I}$ value higher than that of CPB itself. In the case of the MBBA-CBP mixture, a non-linear complex, which is not liquid crystalline, may be formed with substantially lower formation constants than those of MBBA-CPB or CPB-ABP. The lack of a long flexible hydrocarbon chain in CBP could cause the decrease in the stability of a complex in the highly ordered liquid crystalline and solid phases. Such an effect is unlikely in the MBBA-CPB and CPB-ABP systems.

Recently, Oh[10] has studied several other binary liquid crystalline systems, where one component bears a cyano group, and reports similar phase diagrams but with extended smectic ranges. He proposes a dipole-induced lamellar structure as an alternate model to explain the phase diagrams. Such a model may indeed be applicable in some situations, particularly in explaining the induced smectic mesomorphism. It is hard to see how such a model could explain the strong non-linearity in $T_{N\to I}$ in the case of the CPB-ABP mixtures studied in this work, where a donor-acceptor interaction appears so likely. Further studies on these unusual phase relationships should allow a mechanistic distinction as well as providing liquid crystals with wider mesomorphic ranges and modified electro-optic parameters.

Acknowledgment: This work was supported by the U. S. Army Research Office (Durham) under Grant No. DAHC04-74-G-0186.

REFERENCES

1. J. W. Park, C. S. Bak and M. M. Labes, J. Am. Chem. Soc., 97, 4398 (1975).
2. J. W. Park and M. M. Labes, J. Appl. Phys., to be published January 1977.
3. J. S. Dave and M. J. S. Dewar, J. Chem. Soc., 4616 (1954); J. Chem. Soc.,4305 (1955); J. S. Dave and K. L. Vasanth, Mol. Cryst. Liq. Cryst., 2, 125 (1966).
4. M. Schadt and F. Müller, J. Chem. Phys., 65, 2224 (1976).
5. P. E. Cladis, J. Rault and J. P. Burger, Mol. Cryst. Liq. Cryst., 13, 1 (1971).
6. H. T. Peterson and D. E. Martire, Mol. Cryst. Liq. Cryst., 25, 89 (1974); D. E. Martire, G. A. Oweimreen,

G. I. Agren, S. G. Ryan and H. T. Peterson, J. Chem. Phys., 64, 1456 (1975).
7. S. A. Shaya and H. Yu, J. Phys. (Paris), 36, C1-59 (1975).
8. 4-aminobiphenyl is known as a carcinogen and must be handled with appropriate care.
9. For details, see J. W. Park, Ph.D. dissertation, Temple University, 1977.
10. C. S. Oh, Abstract C1-31, Sixth International Liquid Crystal Conference, Kent, Ohio, August 1976.

A NEW GENERATION PROCESS AND MATRIX REPRESENTATION OF DISCLINATIONS IN NEMATIC AND CHOLESTERIC LIQUID CRYSTALS+

A. E. Stieb* and M. M. Labes

Department of Chemistry, Temple University, Philadelphia, Pa. 19122

Abstract

Disclinations in nematic liquid crystals are described as transitions between two different states of quantized bulk deformations in a layer. The quantized states of deformation are due to well defined uniform boundary conditions, which allow only discrete solutions of the partial Euler differential equations governing the deformation.

A new continuous generation process for the non-singular disclinations of integer strength is discussed. The local turns of the director field, involved in this process, can be used for an algebraic description of the topological properties of the disclinations. This formalism can also be applied to disclinations of half integer strength and to disclinations in cholesteric liquid crystals. From this theory, the existence of stable disclinations of the strength $s=0$ can be predicted.

Disclinations of integer strength are created by an experimental process analogous to the new theoretical generation process. Experimental evidence for the existence of disclinations of the strength 0 is given.

*Visiting Research Associate, 1975-1976. Permanent address: Institut f. Ang. Festkörper-Physik, 7800 Freiburg, W. Germany

Fluorescent Liquid Crystal Display Utilizing an Electric Field Induced Cholesteric-Nematic Transition*

L. J. Yu and M. M. Labes

Department of Chemistry, Temple University, Philadelphia, PA 19122

Abstract

An electric-field induced cholesteric-nematic transition on a sample containing a europium chelate guest molecule of little or no polarization shows contrast ratios as high as 9:1 for its brilliant red (612 nm) fluorescence.